ADP-11-44/T766, YITP-11-104, J-PARC-TH-003

arXiv:1202.2299v1 [hep-ph] 10 Feb 2012

Valence quark and meson cloud contributions for the $\gamma^*\Lambda \to \Lambda^*$ and $\gamma^*\Sigma^0 \to \Lambda^*$ reactions

G. Ramalho[1], D. Jido[2,3], and K. Tsushima[4]

[1]*CFTP, Instituto Superior Técnico, Universidade Técnica de Lisboa, Av. Rovisco Pais, 1049-001 Lisboa, Portugal*
[2]*Yukawa Institute for Theoretical Physics, Kyoto University, Kyoto 606-8502, Japan*
[3]*J-PARC Branch, KEK Theory Center, Institute of Particle and Nuclear Studies,*
High Energy Accelerator Research Organization (KEK),
203-1, Shirakata, Tokai, Ibaraki, 319-1106, Japan and
[4]*CSSM, School of Chemistry and Physics, University of Adelaide, Adelaide SA 5005, Australia*

(Dated: February 13, 2012)

We estimate the valence quark contributions for the $\gamma^*Y \to \Lambda^*$ ($Y = \Lambda, \Sigma^0$) electromagnetic transition form factors. We focus particularly on the case $\Lambda^* = \Lambda(1670)$ as an analog reaction with $\gamma^*N \to N(1535)$. The results are compared with those obtained from chiral unitary model, where the Λ^* resonance is dynamically generated and thus the electromagnetic structure comes directly from the meson cloud excitation of the baryon ground states. The form factors for the case $Y = \Sigma^0$ in particular, depend crucially on the two real phase (sign) combination, a phase between the Λ and Λ^* states, and the other, the phase between the Λ and Σ^0 radial wave functions. Depending on the combination of these two phases, the form factors for the $\gamma^*\Sigma^0 \to \Lambda^*$ reaction can be enhanced or suppressed. Therefore, there is a possibility to determine the phase combination by experiments.

I. INTRODUCTION

With the development of the modern accelerators the study of the meson and light baryon structure has been becoming one of the most exciting topics in physics. Although the underlying theory of strong interaction, quantum chromodynamincs (QCD), is known for a long period, its complexity in low energy region forces us to use some effective theories (aside from lattice QCD), either based on the quark and gluon degrees of freedom, or some effective interactions between the mesons and baryons. Among the various possible meson-baryon reactions, the reactions that involve strangeness are particularly interesting, due to the accessibility of the modern accelerators to strange particles such as kaons, K, antikaons, $\bar{K}$, and hyperons, Σ and Λ.

In this study we focus on the electromagnetic excitations of Λ hyperon ground state. The Λ ground state, $\Lambda(1116)$ is $J^P = \frac{1}{2}^+$ and belongs to the spin 1/2 octet baryon multiplet, in which also the nucleons belong. The lowest mass of the Λ excited state (Λ^*) reported by the particle data group [1] is $\Lambda(1405)$, a $J^P = \frac{1}{2}^-$ state. The $\Lambda(1405)$ state has collected a lot of interests over the years for the reasons following: (i) it has been suggested as a dynamically generated state (molecular-like state) composed largely of the $\pi\Sigma$ and $\bar{K}N$ states [2–5]; (ii) it is difficult to classify in terms of naive quark models based on $SU(6)$ symmetry. In the representation of spin-flavor $SU(6)$ symmetry the $\Lambda(1405)$ state can be a mixture of three distinct 3-quark states including the Λ-singlet state [6–8]. However, its mass is difficult to predict in Karl-Isgur model [8], as well as in cloudy bag model (CBM) [9]. In CBM the $\Lambda(1405)$ was interpreted primarily as a $\bar{K}N$ bound state [9]. Thus, there is a strong indication that the $\Lambda(1405)$ is a dynamically generated meson-baryon molecular-like state with a single or a double pole structure [9–19]. In particular, it was demonstrated that the $\Lambda(1405)$ is composed substantially of the meson-baryon components within the chiral unitary model [13]. Nevertheless, there are some works that support the $\Lambda(1405)$ as a 3-quark state [20–22].

Therefore, to study the $\gamma^*\Lambda \to \Lambda^*$ reaction is very interesting also by the reasons following. In one aspect this reaction has a possible analogy with the $\gamma^*N \to N^*(1535)$ reaction. Because $\gamma^*\Lambda \to \Lambda^*$ is a transition between a $J^P = \frac{1}{2}^+$ and a $J^P = \frac{1}{2}^-$ states, we have a possibility to interpret the $\Lambda(1405)$ as a p-state excitation of one quark in the ground state $\Lambda(1116)$, analogous to $N^*(1535)$, a p-state excitation of the nucleon [23]. However, the $\Lambda(1405)$ has considerably lower mass than $N^*(1535)$. Furthermore, it has a larger mass difference with the nearest d-state partner $\Lambda(1520)$ compared to the case of $N^*(1535)$ and $N^*(1520)$. The mass order is even reversed for the $\Lambda(1405)$ case. Because of the reasons discussed above, it is very difficult to interpret naively $\Lambda(1405)$ as a simple p-state excitation of $\Lambda(1116)$.

Searching for the next higher mass excited state of $\Lambda(1116)$ with $J^P = \frac{1}{2}^-$, one finds $\Lambda(1670)$, which can be an analogous with S_{11} excitation of the nucleon, $N^*(1535)$. Since Σ^0 is the neutral Σ ground state ($J^P = \frac{1}{2}^+$) which belongs to the spin 1/2 octet baryon multiplet, and the $\gamma^*\Sigma^0 \to \Lambda^*$ reaction is similar to the $\gamma^*\Lambda \to \Lambda^*$ reaction, we also focus on the $\gamma^*\Sigma^0 \to \Lambda^*$ reaction in this study. Because the $\Lambda(1116)$ and $\Sigma^0(1193)$ are similar in masses, the two reactions differ mainly in the initial state quark configurations. As for the other interesting aspect, we note that the $\Lambda(1670)$ resonance can also be described as a dynamically generated meson-baryon state [18, 19], and the $\gamma^* Y \to \Lambda^*$ transition form factors for $Y = \Lambda, \Sigma^0$, were calculated in chiral unitary model [17].

In the previous works, a valence quark model was applied to study the $\gamma^* N \to N^*(1535)$ reaction, and the corresponding transition form factors and helicity amplitudes were studied [23, 24]. The reaction was also studied in a coupled-channels chiral dynamics (chiral unitary model) [25]. In the chiral unitary model the contributions for the transition form factors come entirely from the meson-baryon states (meson cloud effect). For the $\gamma^* N \to N^*(1535)$ reaction the transition form factors F_1^* (Dirac-type) and F_2^* (Pauli-type) can be expressed in terms of the transverse ($A_{1/2}$) and longitudinal ($S_{1/2}$) helicity amplitudes [23, 26]. In Ref. [23], it was found that the F_1^* can be explained very well just taking into account the valence quark effect. By contrast, the meson cloud seems to play a very important role for the F_2^*, in particular in the low Q^2 region [25]. Then, such different roles between the valence quark and meson cloud effects may be reflected in the experimentally extracted helicity amplitudes $S_{1/2}$ and $A_{1/2}$. This possibility was indeed demonstrated in Ref. [24]. We will briefly review also these results.

Therefore, one of our main motivations of this study is to investigate whether or not the different roles of the valence quark and meson cloud effects observed for the $\gamma^* N \to N^*(1535)$ reaction, can also be observed in the $\gamma^* Y \to \Lambda^*$ reactions with $Y = \Lambda$ and Σ^0. In particular, we focus on the structure of $\Lambda(1670)$ in this study. Assuming that $\Lambda(1670)$ is a radial p-state excitation of $\Lambda(1116)$, we estimate the valence quark contributions for the $\gamma^* Y \to \Lambda^*$ transition form factors as well as the helicity amplitudes. For this purpose, we use the covariant spectator quark model [23, 27–29], which was successfully applied to the study of the $\gamma^* N \to N^*(1535)$ reaction. The results of the covariant spectator quark model for the $\gamma^* Y \to \Lambda^*$ reaction are also compared with those obtained with the chiral unitary model [17], where the Λ^* is generated as a meson-baryon molecular-like state such as the $N\bar{K}$, $\Lambda\eta$ and ΞK states. Then, one of the interests is the structure of the $\Lambda(1670)$ state, namely, how it can be interpreted, either it is predominantly a meson-baryon molecular-like state, or dominated by the 3-valence-quark state. Furthermore, we also show that the $\gamma^* \Sigma^0 \to \Lambda^*$ transition form factors depend crucially on the combination of the two unknown real phases (signs), a phase between the Λ and Λ^* three-quark wave functions (to be denoted by η_{Λ^*}), and a phase between the Λ and Σ^0 wave functions (to be denoted by $\eta_{\Lambda\Sigma^0}$).

This article is organized as follows. In Sec. II we define the $\gamma^* Y \to \Lambda^*$ ($Y = \Lambda, \Sigma^0$) transition form factors, and their relations with the helicity amplitudes. In Sec. III we present the covariant spectator quark model and estimate the valence quark contributions for $\gamma^* Y \to \Lambda^*$ ($Y = \Lambda, \Sigma^0$). We discuss in Sec. IV the $\Lambda(1670)$ state based on the chiral unitary model, and estimate the contributions from the meson-baryon states in the $\gamma^* Y \to \Lambda^*$ ($Y = \Lambda, \Sigma^0$) reactions. In Sec. V we present the results from the both models, and give discussions. Finally in Sec. VI we give conclusions of the present study.

II. FORM FACTORS AND HELICITY AMPLITUDES

The $\gamma^* Y \to \Lambda^*$ electromagnetic transition current for Y a strangeness $S = -1$ and $J^P = \frac{1}{2}^+$ state, and Λ^* a $J^P = \frac{1}{2}^-$ excited state of the Λ ground state ($J^P = \frac{1}{2}^+$), can be represented as [23, 26]

$$J_Y^\mu = e\left[\left(\gamma^\mu - \frac{\not{q} q^\mu}{q^2}\right) F_1^Y(Q^2) + \frac{i\sigma^{\mu\nu} q_\nu}{M_{\Lambda^*} + M_Y} F_2^Y(Q^2)\right]\gamma_5, \tag{1}$$

where F_i^Y ($i = 1, 2$) are the transition form factors, and q the four-momentum transfer (defined below) with $Q^2 = -q^2$. The factor e is the absolute electron charge given by $e = \sqrt{4\pi\alpha}$ with α being the electromagnetic fine structure constant. Note that the form factors are frame independent since Eq. (1) is Lorentz covariant. We are particularly interested in the cases $Y = \Lambda$ and Σ^0 in this study.

The current J_Y^μ can be projected on the initial state $u_Y(P_-, S_z)$ and final state $\bar{u}_{\Lambda^*}(P_+, S_z')$ Dirac spinors, where P_- (P_+) is the initial (final) momentum, $q = P_+ - P_-$, and S_z (S_z') the spin projection.

More familiar matrix elements may be the helicity amplitudes. In this case the current J_Y^μ is projected on the photon polarization states $\epsilon_\mu^{(\lambda)}$, where the polarizations can be longitudinal ($\lambda = 0$) or transverse ($\lambda = \pm$). As the photon polarizations depend on the frame the helicity amplitudes are frame dependent. The most common choice of the reference frame is the final state rest frame, Λ^* at rest. In this frame we can define the transverse ($A_{1/2}^Y$) and longitudinal ($S_{1/2}^Y$) helicity amplitudes as [26]

$$A_{1/2}^Y = \sqrt{\frac{2\pi\alpha}{K}}\frac{1}{e}\left\langle \Lambda^*, S_z' = +\frac{1}{2}\right|\epsilon^{(+)}\cdot J_Y\left|Y, S_z = -\frac{1}{2}\right\rangle, \tag{2}$$

$$S_{1/2}^Y = \sqrt{\frac{2\pi\alpha}{K}}\frac{1}{e}\left\langle \Lambda^*, S_z' = +\frac{1}{2}\right|\epsilon^{(0)}\cdot J_Y\left|Y, S_z = +\frac{1}{2}\right\rangle\frac{|\mathbf{q}|_Y}{Q}, \tag{3}$$

with $\alpha = \frac{e^2}{4\pi}$, and

$$K = \frac{M_{\Lambda^*}^2 - M_Y^2}{2M_{\Lambda^*}}. \tag{4}$$

In the above $|\mathbf{q}|_Y$ is the absolute value of the photon three-momentum $\mathbf{q}$ in the Λ^* rest frame,

$$|\mathbf{q}|_Y = \frac{\sqrt{[(M_{\Lambda^*} + M_Y)^2 + Q^2][(M_{\Lambda^*} - M_Y)^2 + Q^2]}}{2M_{\Lambda^*}}. \tag{5}$$

The subindex Y is to label the initial state.

In the Λ^* rest frame we can relate the helicity amplitudes with the form factors [26]:

$$A^Y_{1/2} = -2b\left[F^Y_1 + \frac{M_{\Lambda^*} - M_Y}{M_{\Lambda^*} + M_Y} F^Y_2\right], \tag{6}$$

$$S^Y_{1/2} = \sqrt{2}b(M_{\Lambda^*} + M_Y)\frac{|\mathbf{q}|_Y}{Q^2}\left[\frac{M_{\Lambda^*} - M_Y}{M_{\Lambda^*} + M_Y} F^Y_1 - \tau F^Y_2\right], \tag{7}$$

with

$$\tau = \frac{Q^2}{(M_{\Lambda^*} + M_Y)^2}, \tag{8}$$

and

$$b = e\sqrt{\frac{(M_{\Lambda^*} + M_Y)^2 + Q^2}{8M_Y(M^2_{\Lambda^*} - M^2_Y)}}. \tag{9}$$

III. SPECTATOR QUARK MODEL

In the spectator formalism [30–32] a baryon is represented as a 3-quark state and the wave function is expressed in terms of the corresponding baryon spin-flavor [27, 29, 33]. Then the baryon system is decomposed as an off-mass-shell constituent quark, free to interact with electromagnetic fields, and two on-mass-shell quarks. Integrating over the on-mass-shell momenta we reduce the baryon to a quark-diquark system which has an effective diquark mass m_D [27, 33, 34].

The electromagnetic interaction with the quark is described in terms of a vector meson dominance (VMD) parametrization (to be described later), that simulates the constituent quark internal structure. The quark structure parameterizes effectively the interactions with gluons and quark-antiquark polarization effects. The quark electromagnetic current was calibrated previously by the nucleon and decuplet baryon data [27, 33], and also tested in the lattice regime for the nucleon elastic reaction as well as for the $\gamma N \to \Delta$ transition [28, 33, 35, 36]. The model was also applied to the physical regime to study the octet baryon and decuplet baryon systems [28, 37–42], and some of the excited states of nucleon and Δ [23, 43, 44].

A. Wave functions

We next discuss the spin-flavor-radial wave functions of the systems relevant in this work, namely, Λ, Σ^0, and Λ^*, where Λ^* is interpreted as a 3-quark excitation of the Λ ground state with negative parity. The structure of the Λ and Σ^0 systems are based on Ref. [28], which studied the octet baryon electromagnetic properties. As for the Λ^*, based on the structure considered for the $N^*(1535)$ in Ref. [23], we generalized it.

1. *Spin-flavor wave functions*

In Ref. [28] it was shown that the octet baryon systems can be described reasonably well in an S-state configuration for the quark-diquark system, and that the same structure of wave function applies for all the members of the octet baryons except for the flavor states. The general structure of the wave function is written by [28]

$$\Psi_Y(P,k) = \frac{1}{\sqrt{2}}\left[\phi^0_S|M_A\rangle_Y + \phi^1_S|M_S\rangle_Y\right]\psi_Y(P,k), \tag{10}$$

where P is the total momentum of particle Y, k the diquark momentum, ψ_Y is the radial wave function, and $\phi^{0,1}_S$ are the spin wave functions. The flavor wave functions are presented in Table I. The spin wave functions (the same for all the octet members) are expressed as [23, 27, 28],

$$\begin{aligned} \phi^0_S &= u_Y(P,S_z),\\ \phi^1_S &= -(\varepsilon^*_P)_\alpha(\lambda_D)U^\alpha_Y(P,S_z), \end{aligned} \tag{11}$$

where U^α_Y is the vector-spinor [27, 40],

$$U^\alpha_Y(P,s) = \frac{1}{\sqrt{3}}\gamma_5\left(\gamma^\alpha - \frac{P^\alpha}{M_Y}\right)u_Y(P,S_z), \tag{12}$$

and $u_Y(P,S_z)$ the Y-Dirac spinor with the spin projection S_z. In Eq. (11), $\varepsilon_P(\lambda_D)$ with $\lambda_D = 0,\pm$ are the spin-1 diquark polarization states defined in the fixed-axis representation as a function of the Y-momentum [27, 45]. For later discussions, we note that, even the flavor states can be well defined, the total wave functions can have sign ambiguities due to the normalization constants for the radial wave functions ψ_Y. Note however, that the sign is not relevant for the elastic reactions like the Λ and Σ electromagnetic form factors, since the results are proportional to the integral with the product of the two (real number) functions ψ_Y, although they have different arguments [28].

As for the Λ^* state with $J^P = \frac{1}{2}^-$, we use the analogy with the $N^*(1535)$ to represent the corresponding wave function. Assuming as in Ref. [23] that the Λ^* is dominated by the internal quark states with a total spin 1/2 and has no P-states inside the diquark (pointlike diquark), it is written by

$$\Psi_{\Lambda^*}(P,k) = \frac{1}{\sqrt{2}}\left[\Phi_\rho|M_A\rangle_\Lambda - \Phi_\lambda|M_S\rangle_\Lambda\right]\psi_{\Lambda^*}(P,k), \tag{13}$$

where Φ_ρ and Φ_λ are the spin states to be defined shortly, and ψ_{Λ^*} the Λ^* radial wave function. Note that the Λ^* and Λ are described by the same flavor wave function (see Table I). The states $\Phi_{\rho,\lambda}$ are defined respectively by [23],

$$\begin{aligned} \Phi_\rho(\pm) &= -\gamma_5\mathcal{N}'_{\Lambda^*}\left[(\varepsilon_0\cdot\tilde{k})u_{\Lambda^*}(\pm) - \sqrt{2}(\varepsilon_\pm\cdot\tilde{k})u_{\Lambda^*}(\mp)\right],\\ \Phi_\lambda(\pm) &= \gamma_5\mathcal{N}'_{\Lambda^*}\left[(\varepsilon_0\cdot\tilde{k})\varepsilon^*_\alpha U^\alpha_{\Lambda^*}(\pm) - \sqrt{2}(\varepsilon_\pm\cdot\tilde{k})\varepsilon^*_\alpha U^\alpha_{\Lambda^*}(\mp)\right], \end{aligned} \tag{14}$$

Y	$\|M_S\rangle_Y$	$\|M_A\rangle_Y$
Λ	$\frac{1}{2}\left[(dsu-usd)+s(du-ud)\right]$	$\frac{1}{\sqrt{12}}\left[s(du-ud)-(dsu-usd)-2(du-ud)s\right]$
Σ^0	$\frac{1}{\sqrt{12}}\left[s(du+ud)+(dsu+usd)-2(ud+du)s\right]$	$\frac{1}{2}\left[(dsu+usd)-s(ud+du)\right]$

TABLE I: Flavor wave functions of Λ and Σ^0.

where $\pm$ hold for the spin projections $S_z = \pm\frac{1}{2}$, and ε_0 is a short notation for $\varepsilon_P(0)$ of the diquark polarization associated with the Λ^*, and $\mathcal{N}'_{\Lambda^*}$ is the normalization factor, and

$$\tilde{k} = k - \frac{P\cdot k}{M_{\Lambda^*}^2}P. \tag{15}$$

This last four-momentum reduces to the diquark three-momentum in the Λ^* rest frame. As for $U^\alpha_{\Lambda^*}$, it is defined by Eq. (12) with $M_Y \to M_{\Lambda^*}$. The normalization factor $\mathcal{N}'_{\Lambda^*}$ can be represented as

$$\mathcal{N}'_{\Lambda^*} = \eta_{\Lambda^*} N, \tag{16}$$

where $N = 1/\sqrt{-\tilde{k}^2}$, and η_{Λ^*} is a relative phase (sign) between the Λ and Λ^* states to be discussed later.

The states Φ_ρ and Φ_λ in Eq. (14) are constructed respectively to be antisymmetric and symmetric for the interchange of the quarks 1 and 2 [23].

2. *Radial wave functions*

Since the baryon and the diquark are on-mass-shell in the spectator quark model, we can represent the baryon radial wave function in term of $(P-k)^2$. We can use then the dimensionless variable,

$$\chi_B = \frac{(M_B - m_D)^2 - (P-k)^2}{M_B m_D}, \tag{17}$$

where M_B is the mass of the baryon B and m_D the diquark mass. Following Ref. [28], we take the form for the Y $(=\Lambda, \Sigma^0)$ wave functions,

$$\psi_Y(P,k) = \frac{\mathcal{N}_Y}{m_D(\beta_1+\chi_Y)(\beta_3+\chi_Y)}, \tag{18}$$

where the values of β_1 and β_3 were fixed in Ref. [28] as $\beta_1 = 0.0440$ and $\beta_3 = 0.7634$, and $\mathcal{N}_Y$ is the normalization constant. We assume that $\mathcal{N}_Y$ is *positive*. While β_1 parameterizes the spacial long-range distribution of the quarks which are dominated by the light quarks, β_3 regulates the short-range structure in a system with only one strange quark. The normalization constant, $\mathcal{N}_Y$, is determined by the condition,

$$\int_k |\psi_Y(\bar{P},k)|^2 = 1, \tag{19}$$

where $\bar{P} = (M_Y, 0, 0, 0)$ is the Y-momentum in its rest frame, and $\int_k$ stands for $\int \frac{d^3\mathbf{k}}{2E_D(2\pi)^3}$, where E_D is the diquark on-mass-shell energy. Note that Eq. (19) only determines the magnitude of $\mathcal{N}_Y$, but not the sign.

For the Λ^* wave function, we take also the form of Eq. (18), except that χ_Y is replaced by χ_{Λ^*}, meaning that the M_Y is replaced by M_{Λ^*}. This choice is equivalent to state that the Λ and Λ^* have the same radial wave function, and they are distinguished only by the spin states. It also means that the normalization constants in the radial wave functions, $\mathcal{N}_\Lambda$ and $\mathcal{N}_{\Lambda^*}$ are equal[1] and therefore have the same sign.

We can now discuss the sign η_{Λ^*} in Eq. (16). Since it is already assumed that the normalization constant of the radial wave function $\mathcal{N}_\Lambda$ is positive, η_{Λ^*} defines the sign of the $\gamma^*\Lambda \to \Lambda^*$ transition form factors. Because we have no clue for the sign of the form factors till the date, we will keep the factor η_{Λ^*} in the following equations. We call also attention that the sign corresponding to the $\gamma^* N \to N^*(1535)$ reaction is equivalent to $\eta_{\Lambda^*} = 1$, where this was determined by the experimentally extracted sign for the form factor F_1^* [23].

B. Electromagnetic transition current

The electromagnetic current for the transition $\gamma^* Y \to \Lambda^*$ in a relativistic impulse approximation is given by [27, 28, 33]

$$J_Y^\mu = 3\,e \sum_\Gamma \int_k \bar{\Psi}_{\Lambda^*}(P_+,k) j_q^\mu \Psi_Y(P_-,k), \tag{20}$$

where $\Gamma = \{s, \lambda_D\}$ (the scalar diquark s, and the vector diquark polarizations $\lambda_D = 0, \pm 1$), and j_q^μ is the quark current operator associated with the quark 3. The factor 3 accounts for the contributions from the quark pairs (13) and (23) [the same contribution as that from the pair (12)].

---

[1] For the radial wave functions with the structure of Eqs. (17) and (18), the normalization condition given by Eq. (19) uses $\chi_B = 2\left(\frac{E_D}{m_D} - 1\right)$, which is independent of the baryon mass. As a consequence, the normalization constant is independent of the baryon mass.

1. Quark current

The quark current j_q^μ (in e units) can be represented as [27, 28, 33, 40, 41]

$$j_q^\mu = j_1 \hat{\gamma}^\mu + j_2 \frac{i\sigma^{\mu\nu}q_\nu}{2M}, \tag{21}$$

where M is the nucleon mass, and

$$\hat{\gamma}^\mu = \gamma^\mu - \frac{\not{q} q^\mu}{q^2}, \tag{22}$$

and j_i $(i = 1, 2)$ are the Dirac and Pauli quark operators, respectively. The inclusion of the term $\not{q} q^\mu / q^2$ in the quark current is equivalent to use the Landau prescription [46, 47] to the final electromagnetic current. The term restores current conservation but does not affect the observables calculated [46].

The operators j_i $(i = 1, 2)$ act on the flavor states $|M_A\rangle_Y$ and $|M_S\rangle_Y$ written in terms of the symmetry with respect to the quark 3. The operators j_i can be decomposed into the sum of $SU(3)$-space operators [28, 33],

$$j_i = \frac{1}{6} f_{i+} \lambda_0 + \frac{1}{2} f_{i-} \lambda_3 + \frac{1}{6} f_{i0} \lambda_s, \tag{23}$$

where $\lambda_0 = \mathrm{diag}(1, 1, 0)$, $\lambda_3 = \mathrm{diag}(1, -1, 0)$ and $\lambda_s = \mathrm{diag}(0, 0, -2)$, and f_{in} $(i = 1, 2,\ n = 0, \pm)$ define the constituent quark form factors. The operators act on the third quark, where the quark wave function is represented by $q = (uds)^T$.

The quark electromagnetic form factors are normalized as $f_{1n}(0) = 1$ $(n = 0, \pm)$, $f_{2\pm}(0) = \kappa_\pm$ and $f_{20}(0) = \kappa_s$. The isoscalar (κ_+) and isovector (κ_-) anomalous magnetic moments are related with the u and d quark anomalous magnetic moments by $\kappa_+ = 2\kappa_u - \kappa_d$ and $\kappa_- = \frac{2}{3}\kappa_u - \frac{1}{3}\kappa_d$ [27]. As for κ_s it is the strange quark anomalous magnetic moment [33, 42].

2. Quark electromagnetic form factors

To parameterize the quark current (23), we adopt the structure inspired by the vector meson dominance (VMD) mechanism as in Refs. [27, 33]:

$$\begin{aligned}
f_{1\pm} &= \lambda_q + (1 - \lambda_q) \frac{m_v^2}{m_v^2 + Q^2} + c_\pm \frac{M_h^2 Q^2}{(M_h^2 + Q^2)^2}, \\
f_{10} &= \lambda_q + (1 - \lambda_q) \frac{m_\phi^2}{m_\phi^2 + Q^2} + c_0 \frac{M_h^2 Q^2}{(M_h^2 + Q^2)^2}, \\
f_{2\pm} &= \kappa_\pm \left\{ d_\pm \frac{m_v^2}{m_v^2 + Q^2} + (1 - d_\pm) \frac{M_h^2}{M_h^2 + Q^2} \right\}, \\
f_{20} &= \kappa_s \left\{ d_0 \frac{m_\phi^2}{m_\phi^2 + Q^2} + (1 - d_0) \frac{M_h^2}{M_h^2 + Q^2} \right\},
\end{aligned} \tag{24}$$

where m_v, m_ϕ and M_h are the masses respectively corresponding to the light vector meson $m_v \simeq m_\rho$, the ϕ meson (associated with an $s\bar{s}$ state), and an effective heavy meson with mass $M_h = 2M$ to represent the short-range phenomenology. For the isoscalar component it should be $m_v = m_\omega$, but we neglect the small mass difference between the ρ and ω mesons, and use m_ρ. The coefficients $c_0, c_\pm$ and $d_0, d_\pm$ were determined in the previous studies of the nucleon (model II) [27] and Ω^- [33]. The values are respectively, $c_+ = 4.160$, $c_- = 1.160$, $d_+ = d_- = -0.686$, $c_0 = 4.427$ and $d_0 = -1.860$ [33]. The parameter $\lambda_q = 1.21$ is fixed to give the correct quark number density in deep inelastic scattering [27].

In this study we use the values of the parameters determined by the study of the octet baryon electromagnetic form factors [28]:

$$\kappa_u = 1.6690, \quad \kappa_d = 1.9287, \quad \kappa_s = 1.4620. \tag{25}$$

With the wave functions (10) and (13) one can write the quantity in Eq. (20) as

$$\begin{aligned}
\sum_\Gamma \bar{\Psi}_{\Lambda^*} j_q^\mu \Psi_Y \; = \; & + \frac{\mathcal{A}}{2} \left\{ j_1^A \bar{\Phi}_\rho \hat{\gamma}^\mu \phi_S^0 + j_2^A \bar{\Phi}_\rho \frac{i\sigma^{\mu\nu}q_\nu}{2M} \phi_S^0 \right\} \\
& - \frac{\mathcal{A}}{2} \left\{ j_1^S \bar{\Phi}_\rho \hat{\gamma}^\mu \phi_S^1 + j_2^S \bar{\Phi}_\rho \frac{i\sigma^{\mu\nu}q_\nu}{2M} \phi_S^1 \right\},
\end{aligned} \tag{26}$$

where

$$\begin{aligned}
j_i^A &= {}_\Lambda\langle M_A | j_i | M_A \rangle_Y, \\
j_i^S &= {}_\Lambda\langle M_S | j_i | M_S \rangle_Y,
\end{aligned} \tag{27}$$

for $i = 1, 2$, and they are the coefficients that encapsulate the flavor effect [28, 33, 41], and $\mathcal{A} = \mathcal{N}'_{\Lambda^*} \psi_{\Lambda^*}(P_+, k) \psi_Y(P_-, k)$. In Eq. (26) the sum in the diquark polarizations λ_D is implicit for the vector diquark contributions (terms in ϕ_S^1).

The calculation of the coefficients $j_i^{A,S}$ $(i = 1, 2)$ gives,

$$j_i^S = \frac{1}{6} f_{i+}, \qquad j_i^A = \frac{1}{18} (f_{i+} - 4 f_{i0}), \tag{28}$$

for the $\gamma^* \Lambda \to \Lambda^*$ reaction, and

$$j_i^S = -\frac{1}{\sqrt{12}} f_{i-}, \qquad j_i^A = \frac{1}{\sqrt{12}} f_{i-}, \tag{29}$$

for the $\gamma^* \Sigma^0 \to \Lambda^*$ reaction. In the case of $\gamma^* \Lambda \to \Lambda^*$ the coefficients are the same as ones calculated in Ref. [28] for the elastic Λ electromagnetic form factors. As for the $\gamma^* \Sigma^0 \to \Lambda^*$ reaction, they are explicitly calculated, and the coefficients are the same as those for the reaction $\gamma^* \Lambda \to \Sigma^0$, and reflect the isovector nature of the reaction [48]. In both reactions, there is no interference between the $|M_A\rangle_Y$ and $|M_S\rangle_Y$ states which are in the initial and final states.

Note that, in the second term in Eq. (26) there is a dependence on the diquark polarization vectors $\varepsilon^\alpha_{P_+}(\lambda_D)$ and $\varepsilon^{\beta *}_{P_-}(\lambda_D)$. As already mentioned, these states are defined according to the fixed-axis representation [45] and depend also on the masses of the final (M_{Λ^*}) and initial (M_Y) states, respectively. Taking into account the sum in the diquark polarization states we have [40, 45],

$$\begin{aligned}
\Delta^{\alpha\beta} &\equiv \sum_{\lambda_D} \varepsilon^{\alpha}_{P_+}(\lambda_D)\varepsilon^{\beta *}_{P_-}(\lambda_D) \\
&= -\left(g^{\alpha\beta} - \frac{P_-^{\alpha} P_-^{\beta}}{P_+ \cdot P_-} \right) \\
&\quad -a\left(P_- - \frac{P_+ \cdot P_-}{M_{\Lambda^*}^2} P_+ \right)^{\alpha} \left(P_+ - \frac{P_+ \cdot P_-}{M_Y^2} P_- \right)^{\beta},
\end{aligned} \tag{30}$$

with

$$a = \frac{M_{\Lambda^*} M_Y}{P_+ \cdot P_- (M_{\Lambda^*} M_Y + P_+ \cdot P_-)}. \tag{31}$$

The calculation of the current (20) is carried out by the reduction from Eq. (26) to the evaluation of a few matrix elements. We present in Appendix A the explicit expressions for these matrix elements.

The final result is given by,

$$\begin{aligned}
J^{\mu}_{Y} &= +e\,\frac{1}{2}(3j_1^A + j_1^S)\mathcal{I}_Y\, \hat{\gamma}^{\mu}\gamma_5 \\
&\quad -e\,\frac{1}{2}(3j_2^A - j_2^S)\mathcal{I}_Y\, \frac{i\sigma^{\mu\nu}q_\nu}{2M}\gamma_5,
\end{aligned} \tag{32}$$

where

$$\mathcal{I}_Y(Q^2) = -\eta_{\Lambda^*}\int_k N(\varepsilon_0 \cdot \tilde{k})\psi_{\Lambda^*}(P_+,k)\psi_Y(P_-,,k). \tag{33}$$

The integral $\mathcal{I}_Y$ is covariant and includes the radial dependence of the wave functions. We call $\mathcal{I}_Y$ the overlap integral.

C. Form factors

Combining Eqs. (1) and (32) with the coefficients in Eq. (28), we obtain the form factors for the $\gamma^*\Lambda \to \Lambda^*$ reaction,

$$F_1^{\Lambda}(Q^2) = \frac{1}{6}\left[f_{1+}(Q^2) - 2f_{10}(Q^2)\right]\mathcal{I}_{\Lambda}, \tag{34}$$

$$F_2^{\Lambda}(Q^2) = \frac{1}{3} f_{20}(Q^2)\frac{M_{\Lambda^*} + M_{\Lambda}}{2M}\mathcal{I}_{\Lambda}. \tag{35}$$

As for the $\gamma^*\Sigma^0 \to \Lambda^*$ reaction, using Eq. (29) and we obtain:

$$F_1^{\Sigma}(Q^2) = -\frac{1}{\sqrt{12}} f_{1-}(Q^2)\mathcal{I}_{\Sigma}, \tag{36}$$

$$F_2^{\Sigma}(Q^2) = +\frac{2}{\sqrt{12}} f_{2-}(Q^2)\frac{M_{\Lambda^*} + M_{\Sigma}}{2M}\mathcal{I}_{\Sigma}. \tag{37}$$

Note that the presence of the factor $2M$ in the form factor expressions, which is a consequence of the quark Pauli current expressed in terms of the nucleon mass M [27, 33] in Eq. (21).

The overlap integral $\mathcal{I}_Y$ can be evaluated in the Λ^* rest frame to give a simple expression [23],

$$\mathcal{I}_Y(Q^2) = \eta_{\Lambda^*}\int_k \frac{k_z}{|\mathbf{k}|}\psi_{\Lambda^*}(P_+,k)\psi_Y(P_-,k), \tag{38}$$

where

$$P_- = (E_Y, 0, 0, -|\mathbf{q}|_Y), \qquad P_+ = (M_{\Lambda^*}, 0, 0, 0), \tag{39}$$

with $E_Y = \sqrt{M_Y^2 + |\mathbf{q}|_Y^2} = \frac{M_{\Lambda^*}^2 + M_Y^2 + Q^2}{2M_{\Lambda^*}}$.

From Eq. (38) we may conclude that the signs of the overlap integrals for $Y = \Lambda$ and $Y = \Sigma$ depend on the relative sign of the Λ and Σ scalar wave functions. Defining the factor,

$$\eta_{\Lambda\Sigma} = \frac{\mathcal{N}_{\Lambda}\mathcal{N}_{\Sigma}}{|\mathcal{N}_{\Lambda}\mathcal{N}_{\Sigma}|}, \tag{40}$$

which gives the relative sign between the Λ and Σ radial wave functions, we can write in the limit $M_\Lambda = M_{\Sigma^0}$ as,

$$\mathrm{sgn}(\mathcal{I}_{\Sigma}) = \eta_{\Lambda\Sigma^0} \times \mathrm{sgn}(\mathcal{I}_{\Lambda}). \tag{41}$$

This result is equivalent to state that the relative sign of the integrals $\mathcal{I}_{\Lambda}$ and $\mathcal{I}_{\Sigma}$ is given by the relative sign of $\mathcal{N}_{\Lambda}$ and $\mathcal{N}_{\Sigma}$ (or $\eta_{\Lambda\Sigma^0}$). Since M_Λ and M_{Σ^0} values are close, it is expected that the relation (41) holds also for a certain region of Q^2. The phase $\eta_{\Lambda\Sigma^0}$ is unknown at present, as the same reason for the sign of the $\gamma^*\Lambda \to \Sigma^0$ transition magnetic moment $\mu_{\Lambda\Sigma^0}$ is unknown [1]. If the sign of $\mu_{\Lambda\Sigma^0}$ is determined, we may be able to fix the sign for the $\gamma^*\Sigma^0 \to \Lambda^*$ transition form factors within the present approach. Therefore, although we will assume $\eta_{\Lambda\Sigma^0} = 1$ in the presentation of our results later, we will also discuss the alternative sign possibility.

For later discussions, it is also important to mention that the integral (33) has a behavior,

$$\mathcal{I}_Y(Q^2) \propto |\mathbf{q}|_Y, \tag{42}$$

for small $|\mathbf{q}|_Y$. Recall that $|\mathbf{q}|_Y$, given by Eq. (5), is the photon three-momentum in the $\gamma^* Y \to \Lambda^*$ reaction in the final Λ^* rest frame. See Appendix C of Ref. [23] for the derivation of the relation (42).

We can now discuss the Q^2 range applicable for the present model. From the definition of the transition form factors (1), we can conclude that the Dirac-type form factor F_1^Y should be zero or vanish when $Q^2 \to 0$. However, in the present case if $M_{\Lambda^*} \neq M_Y$, it results to $F_1^*(0) \neq 0$. That is a simple consequence of the relation (42), from what we can conclude that $\mathcal{I}_Y(0) \neq 0$ in the case $Q^2 = 0$, when $|\mathbf{q}|_Y = |\mathbf{q}|_{0Y} = \frac{M_{\Lambda^*}^2 - M_Y^2}{2M_{\Lambda^*}}$. This result is equivalent with that the Y and Λ^* states are not orthogonal in the spectator quark model[2]. The two states would be orthogonal only in the case $M_{\Lambda^*} = M_Y$, when $|\mathbf{q}|_{0Y} = 0$. We can regard the states are approximately orthogonal when $|\mathbf{q}|_{0Y}$ is very small, which leads to $\mathcal{I}_Y(0) \approx 0$. Then, we can assume that the condition $\mathcal{I}_Y(0) \simeq 0$ is satisfied when $Q^2 \gg |\mathbf{q}|_{0Y}^2$.

Interpreting Λ^* as $\Lambda(1670)$ ($M_{\Lambda^*} \simeq 1.670$ GeV) the model is then applicable when $Q^2 \gg |\mathbf{q}|_0^2 = 0.21$ GeV^2 ($M_\Lambda = 1.116$ GeV) for the reaction involving the Λ, and when $Q^2 \gg |\mathbf{q}|_0^2 = 0.17$ GeV^2 ($M_{\Sigma^0} = 1.193$ GeV) for the reaction involving the Σ^0.

IV. CHIRAL UNITARY MODEL

In this section, we briefly explain the description of the $\Lambda(1670)$ resonance and the calculation of the corresponding form factors in the chiral unitary approach. Here we consider the model presented in Refs. [17, 18].

A. Description of $\Lambda(1670)$

In the chiral unitary model, the $\Lambda(1670)$ is dynamically generated in s-wave meson-baryon scattering in the coupled channels of $\bar{K}N$, $\pi\Sigma$, $\eta\Lambda$, $K\Xi$, $\pi\Lambda$ and $\eta\Sigma$ with zero total charge. Here we take small isospin breaking into account in the masses of the mesons and baryons. The s-wave scattering amplitude in these channels is calculated with the scattering equation given by

$$T(W) = V(W) + V(W)G(W)T(W), \tag{43}$$

where W is the center of mass energy of the two-body system. Based on the N/D method with neglecting the left-hand cut, a solution of the scattering equation can be obtained by a simple algebraic equation [19]

$$T = (1 - VG)^{-1}V. \tag{44}$$

For the interaction kernel V in Eq. (44) we take the lowest order of the chiral perturbation theory, which is the Weinberg-Tomozawa term, as

$$V_{ij} = -C_{ij}\frac{1}{4f^2}(2W - M_i - M_j)N_iN_j, \tag{45}$$

with the coupling strength C_{ij}, the meson decay constant f being fixed as $f = 1.123 f_\pi$ with $f_\pi = 93$ MeV, the baryon mass M_i and the normalization of baryon state $N_i \equiv \sqrt{(M_i + E_i)/(2M_i)}$ where E_i is the baryon energy in the c.m. frame. It is important to note that the coupling strength C_{ij} is fixed solely by the flavor $SU(3)$ group structure of the channel, and thus once we fix the meson decay constant, there are no free parameters in the interaction (45). We do not include an explicit pole term in the interaction. This is the reason that the obtained resonance in the scattering amplitude is called a dynamically generated resonance.

The diagonal matrix G in Eq. (44) is the meson-baryon loop function given by

$$G_i(W) = i\int\frac{d^4p}{(2\pi)^4}\frac{2M_i}{p^2 - M_i^2 + i\epsilon}\frac{1}{(P-p)^2 - m_i^2 + i\epsilon}, \tag{46}$$

with the c.m. energy $P = (W, 0, 0, 0)$ and the meson mass m_i. The divergent loop function can be calculated in an analytic form using dimensional regularization, which isolates the divergent part from the integral. The remaining finite constant being called a_i is determined phenomenologically by experiments. Here we use the threshold branching ratios of K^-p to $\pi\Lambda$ and $\pi\Sigma$ observed by stopped K^- mesons in hydrogen [49, 50]. In this study use the following a_i constants determined in Ref. [18]:

$$\begin{aligned} a_{\bar{K}N} &= -1.84, & a_{\pi\Sigma} &= -2.00, & a_{\pi\Lambda} &= -1.83, \\ a_{\eta\Lambda} &= -2.25, & a_{\eta\Sigma} &= -2.38, & a_{K\Xi} &= -2.67, \end{aligned} \tag{47}$$

with the scale of the dimensional regularization $\mu = 630$ MeV.

Since the obtained amplitude is written in an analytic form, we can perform analytic continuation to the complex energy plain to look for resonances poles in the second Riemann sheet. The pole position for the $\Lambda(1670)$ resonance in this model can be found at

$$z = 1680 - 20i \text{ [MeV]}. \tag{48}$$

We also obtain the coupling strength $g_{\Lambda^*}^i$ of the $\Lambda(1670)$ to the channel i as a residue of the scattering amplitude at the resonance pole. The values of the couplings are given in Ref. [17]. The couplings characterize the structure of the $\Lambda(1670)$. The $\Lambda(1670)$ has large couplings to the $\eta\Lambda$ and $K\Xi$ channels. As discussed in Ref. [13] the values of the constants a_i are very important for the nature of the dynamically generated resonance. If we take the constants a_i determined in the natural renormalization scheme which excludes the CDD pole contributions [13], we obtain a resonance pole at $1700 - 21i$ MeV [17]. This is not so different from the pole position (48) determined phenomenologically by the K^-p threshold branching ratios. This means that the resonance obtained in this parameter set is composed mostly by meson-baryon components.

B. Transition amplitude

We calculate the transition amplitude of the $\Lambda(1670)$ resonance using the method developed in Ref. [25]. In the following we adopt an alternative parametrization for the transition current to Eq. (1) as given in Ref. [17]:

---

[2] This is a consequence of the fact that we cannot have simultaneously the Y and Λ^* at rest when $Q^2 = 0$, unless the particles have the same masses. Considering for instance Λ^* at rest in the following. According to Eq. (39), one gets $P_+ = (M_{\Lambda^*}, 0, 0, 0)$, but $P_- = \left(\frac{M_{\Lambda^*}^2 + M_Y^2}{2M_{\Lambda^*}}, 0, 0, -|\mathbf{q}|_{0Y}\right)$. Therefore Y is not at rest.

$$J^\mu_{Y,\mathrm{NR}} = \mathcal{M}^{\mathrm{NR}}_1 \sigma^\mu + \mathcal{M}^{\mathrm{NR}}_2 P^\mu_+ \sigma\cdot q + \mathcal{M}^{\mathrm{NR}}_3 q^\mu \sigma\cdot q, \quad (49)$$

where $\sigma^\mu = (0, \boldsymbol{\sigma})$ with the Pauli matrix σ^i for the hyperon spin space and $P^\mu_+ = (M_{\Lambda^*}, 0, 0, 0)$ and q^μ are the Λ^* and photon momenta, respectively. The current $J^\mu_{Y,\mathrm{NR}}$ is projected on the Y and Σ^0 Pauli spinors. This representation is equivalent to the transition current J^μ_Y of Eq. (1) once one understands that the spin projection on the asymptotic state Dirac spinors $u_Y(P_-, S_z)$ and $\bar{u}_{\Lambda^*}(P_+, S'_z)$ is already performed in the Λ^* rest frame (39). The index NR is intend to indicate that we will make a non-relativistic reduction of the operators and take the leading order contributions, but still the current itself is covariant. The parametrization (49) together with the gauge invariance condition,

$$\mathcal{M}^{\mathrm{NR}}_1 + \mathcal{M}^{\mathrm{NR}}_2 q\cdot P_+ + \mathcal{M}^{\mathrm{NR}}_3 q^2 = 0, \quad (50)$$

is equivalent to the representation of Eq. (1).

With these amplitudes the transition form factors are written as

$$\begin{aligned} F^Y_1(Q^2) &= Q^2 \frac{1}{e}\sqrt{\frac{1}{1+\tau}}\sqrt{\frac{M_Y}{M_{\Lambda^*}}} \\ &\quad \times \left(\frac{M_{\Lambda^*}}{M_Y + M_{\Lambda^*}}\mathcal{M}^{\mathrm{NR}}_2 + \mathcal{M}^{\mathrm{NR}}_3\right), \quad (51) \\ F^Y_2(Q^2) &= (M_Y + M_{\Lambda^*})^2 \frac{1}{e}\sqrt{\frac{1}{1+\tau}}\sqrt{\frac{M_Y}{M_{\Lambda^*}}} \\ &\quad \times \left(-\frac{M_{\Lambda^*}}{M_Y + M_{\Lambda^*}}\mathcal{M}^{\mathrm{NR}}_2 + \tau\mathcal{M}^{\mathrm{NR}}_3\right), (52) \end{aligned}$$

where τ is given by Eq. (8), M_Y and M_{Λ^*} are the masses of the hyperon Y and Λ^*, respectively, and we set[3] $M_{\Lambda^*} = 1670$ MeV. In the above equations, the factor $\frac{1}{e}$ must be included since the form factors defined by (1) are defined without e and the transition amplitudes $\mathcal{M}^{\mathrm{NR}}_i$ include the factor e as shown next. The absolute phases of F^Y_1 and F^Y_2 are arbitrary in the present model. Here we define the phases of the transition form factors obtained in the chiral unitary model so that the value of $A^Y_{1/2}(Q^2)$ at $Q^2 = 0$ for each hyperon Y should be real and positive. This is equivalent to set the value of $F^Y_2(0)$ real and negative from Eq. (6) with $F^Y_1(0) = 0$ thanks to gauge invariance.

The transition amplitudes $\mathcal{M}^{\mathrm{NR}}_i$ are calculated based on the Feynman diagrams shown in Fig. 1 in a nonrelativistic formulation in which the operators are expanded in terms of $1/M_i$ and only the leading contributions are taken. The amplitudes are decomposed in terms of the Lorentz structures given by Eq. (49). As shown in Eqs. (51) and (52), the transition form factors can be expressed by $\mathcal{M}^{\mathrm{NR}}_2$ and $\mathcal{M}^{\mathrm{NR}}_3$. Since it was found in Ref. [25] that the diagram (c) has only $\mathcal{M}^{\mathrm{NR}}_1$ term, which is irrelevant for the form factors, we can actually omit the diagram (c) for the present purpose. It should be noted that the amplitudes $\mathcal{M}^{\mathrm{NR}}_2$ and $\mathcal{M}^{\mathrm{NR}}_3$ remain finite although each process contains one-loop integral. Since the diagram (b) has the γBB vertex having the $1/M_i$ factor, the diagram (b) gives only sub-leading contribution in the nonrelativistic limit and we neglect the diagram (b).

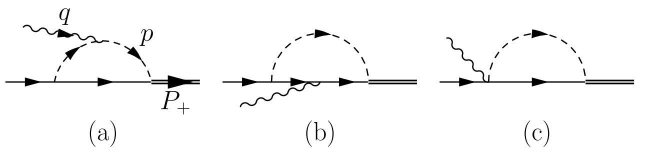

FIG. 1: Feynman diagrams for the phototransition to the Λ^*. The solid, dashed, wavy and double lines denote octet baryons, mesons, photon and Λ^*, respectively. The diagram (b) gives sub-leading contribution in the nonrelativistic limit.

Each vertex in the diagrams is given by the chiral effective theory. The basic interactions of the mesons and baryons are given by the chiral Lagrangian:

$$\begin{aligned} \mathcal{L}_{MBB} &= -\frac{D}{\sqrt{2}f}\,\mathrm{Tr}\left[\bar{B}\gamma_\mu\gamma_5\{\partial^\mu\Phi, B\}\right] \\ &\quad -\frac{F}{\sqrt{2}f}\,\mathrm{Tr}\left[\bar{B}\gamma_\mu\gamma_5[\partial^\mu\Phi, B]\right], \quad (53) \end{aligned}$$

with the meson and baryon fields, Φ and B, defined by

$$\Phi = \begin{pmatrix} \frac{1}{\sqrt{2}}\pi^0 + \frac{1}{\sqrt{6}}\eta & \pi^+ & K^+ \\ \pi^- & -\frac{1}{\sqrt{2}}\pi^0 + \frac{1}{\sqrt{6}}\eta & K^0 \\ K^- & \bar{K}^0 & -\frac{2}{\sqrt{6}}\eta \end{pmatrix}, \quad (54)$$

$$B = \begin{pmatrix} \frac{1}{\sqrt{2}}\Sigma^0 + \frac{1}{\sqrt{6}}\Lambda & \Sigma^+ & p \\ \Sigma^- & -\frac{1}{\sqrt{2}}\Sigma^0 + \frac{1}{\sqrt{6}}\Lambda & n \\ \Xi^- & \Xi^0 & -\frac{2}{\sqrt{6}}\Lambda \end{pmatrix}. (55)$$

The meson-baryon coupling constants are obtained from the Lagrangian as $g^i_A/(2f)$ with the axial coupling constant g^i_A given by D and F together with the Clebsch-Gordan coefficients. The parameters are fixed as

$$D = 0.85 \pm 0.06\ , \qquad F = 0.52 \pm 0.04\ , \quad (56)$$

so as to reproduce the observed axial vector coupling for the octet baryons. The photon couplings to mesons and baryons are given by the gauge coupling:

$$\begin{aligned} \mathcal{L}_{\gamma B} &= -e\mathrm{Tr}\left[\bar{B}\gamma_\mu[Q_{\mathrm{ch}}, B]\right]A^\mu, \quad (57) \\ \mathcal{L}_{\gamma M} &= ie\mathrm{Tr}\left[\partial_\mu\Phi[Q_{\mathrm{ch}}, \Phi]\right]A^\mu, \quad (58) \end{aligned}$$

with the charge matrix $Q_{\mathrm{ch}} = \mathrm{diag}(\frac{2}{3}, -\frac{1}{3}, -\frac{1}{3})$ and $e > 0$. The Kroll-Ruderman terms of the γMBB couplings are obtained by replacing the derivative acting on the meson fields $\partial_\mu \Phi$ with the covariant derivative $D_\mu \Phi = \partial_\mu \Phi + ieA_\mu [Q_{\rm ch}, \Phi]$ in the Lagrangian (53). The Λ^* coupling to the meson and baryon has an s-wave form

---

[3] In the previous work [17], $M_{\Lambda^*} = 1680$ MeV was used. This value corresponds to the real part of the pole position for the $\Lambda(1670)$ in the present model.

$$\mathcal{L}_{\Lambda^* M_i B_i} = g^i_{\Lambda^*} \bar{\Lambda}^* \Phi_i B_i \ , \tag{59}$$

with the coupling constant $g^i_{\Lambda^*}$ determined by the chiral unitary model. The explicit values are given in Ref. [17].

The amplitude given by $-it = J \cdot \epsilon$ for the diagram (a) with channel i is calculated as

$$\begin{aligned} -it^i_a \ &= \ iQ_M A_i \int \frac{d^4p}{(2\pi)^4} \frac{(p-q)\cdot\sigma\,(2p-q)\cdot\epsilon}{(P_+ - p)^2 - M_i^2 + i\epsilon} \\ &\times \frac{1}{(p^2 - m_i^2 + i\epsilon)((p-q)^2 - m_i^2 + i\epsilon)}, \end{aligned} \tag{60}$$

with Q_M the meson (M) charge and A_i is given by $A_i = g^i_A g^i_{\Lambda^*} M_i / f$. After some algebra shown in Ref. [17, 25], we obtain

$$\begin{aligned} -it^i_a \ &= \ iQ_M A_i 2 \int_0^1 dx \int_0^x dy \int \frac{d^4p}{(2\pi)^4} \frac{(p + (y-1)q)\cdot\sigma}{(p^2 - S^i_a + i\epsilon)^3} \\ &\times (2p + (2y-1)q + 2(1-x)P_+)\cdot\epsilon \ , \end{aligned} \tag{61}$$

where S^i_a is defined by

$$\begin{aligned} S^i_a \ &= \ 2P_+ \cdot q(1-x)y - M^2_{\Lambda^*} x(1-x) - q^2 y(1-y) \\ &+ M_i^2 (1-x) + m_i^2 x \ . \end{aligned} \tag{62}$$

In Eq. (61), only even powers of p give contribution after performing the integration. The $\mathcal{M}_2^{\rm NR}$ and $\mathcal{M}_3^{\rm NR}$ amplitudes can be calculated as finite numbers. After performing the integration, we get the $\mathcal{M}_2^{\rm NR}$ and $\mathcal{M}_3^{\rm NR}$ components for the channel i as

$$\mathcal{M}^{i({\rm NR})}_{2a} \ = \ \frac{Q_M A_i}{(4\pi)^2} \int_0^1 dx \int_0^x dy \frac{2(y-1)(1-x)}{S^i_a - i\epsilon}, \tag{63}$$

$$\mathcal{M}^{i({\rm NR})}_{3a} \ = \ \frac{Q_M A_i}{(4\pi)^2} \int_0^1 dx \int_0^x dy \frac{(y-1)(2y-1)}{S^i_a - i\epsilon}. \tag{64}$$

In order to take into account the charge distribution of the constituent mesons and baryons, we multiply the transition amplitudes obtained above by the electromagnetic form factors of the mesons or baryons to which the photon couples. The Q^2 dependence of the helicity amplitude of the Λ^* resonance, thus, stems from the form factors of the meson and baryons components and the intrinsic Q^2 structure of the loops. For the mesons and baryons form factors, we take monopole form factors:

$$F(Q^2) = \frac{\Lambda^2}{\Lambda^2 + Q^2}, \tag{65}$$

with

$$\Lambda_\pi \ = \ 0.727 \ [\text{GeV}], \tag{66}$$

$$\Lambda_K \ = \ 0.828 \ [\text{GeV}], \tag{67}$$

which are determined by the radii of the mesons. These values correspond to $\langle r^2 \rangle = 0.44$ fm^2 and $\langle r^2 \rangle = 0.34$ fm^2 for the pion and the kaon, respectively. For the baryon, we take the same form factor as for the corresponding meson to keep gauge invariance. Thanks to the practically negligible effect of the baryon terms, the approximation made there has no practical consequences.

V. RESULTS

We first present the results of the valence quarks (spectator quark model) and meson cloud (chiral unitary model) for the $\gamma^* N \to N^*(1535)$ transition form factors in the charge +1 channel (namely for the proton target case). Although some of the results were already reported in the previous works [23, 25], we present again some results of the form factors, since they are important and can make the later discussions clearer.

After analyzing the results for the $\gamma^* N \to N^*(1535)$ reaction, we will discuss the reaction $\gamma^* Y \to \Lambda^*$ for $Y = \Lambda$ and Σ^0. The results of the $\gamma^* Y \to \Lambda^*$ reactions will be compared with those of the $\gamma^* N \to N^*(1535)$.

We recall that the applicable region of the present valence quark model is $Q^2 \gtrsim 1$ GeV^2. As for the chiral unitary model, we cannot extend the results for an arbitrary large Q^2, because the amplitudes are calculated using the vertex given by the chiral perturbation theory. Therefore, we expect the results of both formalisms can be compared in the region $Q^2 = 1-2$ GeV^2, where the correlation between the two effects can possibly determine the final result for the transition form factors.

About the chiral unitary model we recall that the contributions from the valence quarks (or baryon core) for the form factors are real numbers. The results from the chiral unitary model are based on a meson-baryon coupled-channels formalism [17, 25] and the states are constructed as a consequence of the meson cloud dressing of the bare octet baryons, and the transition amplitudes are calculated by photon couplings to the hadron constituents. In the diagrams with the baryon dressing (see Fig. 1) one can have on-mass-shell states for the mesons or baryons, therefore the amplitudes and the form factors become complex number functions. As we have already mentioned, the absolute phase is fixed so as to make $A_{1/2}$ to be real and positive, or equivalently F_2 real and negative, at $Q^2 = 0$.

A. $\gamma^* N \to N^*(1535)$ form factors

The results of the covariant spectator quark model and the chiral unitary model for the $\gamma^* N \to N^*(1535)$ transition form factors are presented in Fig. 2. The individual results for the helicity amplitudes were presented in Ref. [23] (for the valence quarks) and in Ref. [25] (for the meson cloud). The results from the covariant spectator quark model are restricted to the region

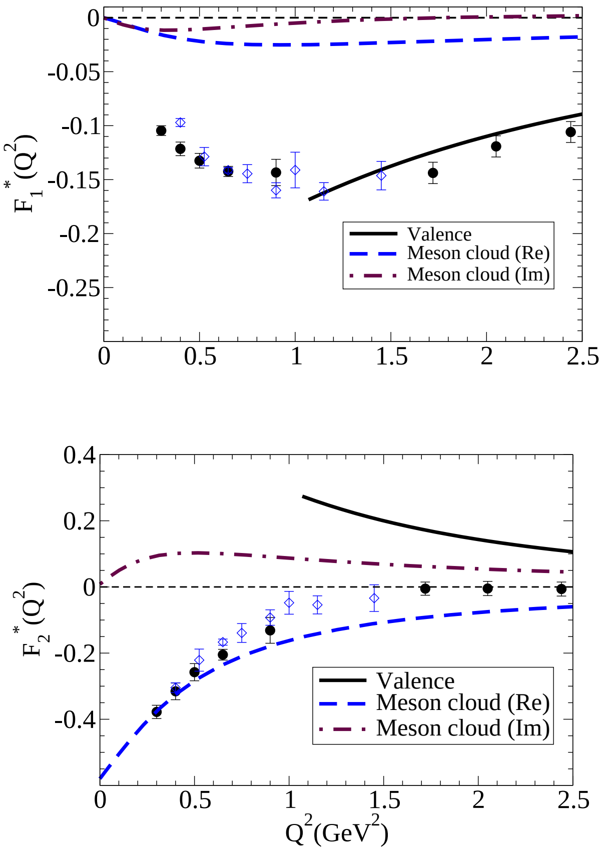

FIG. 2: (Color online) Valence quark and meson cloud contributions for the $\gamma^* N \to N^*(1535)$ transition form factors, $F_1^*(Q^2)$ and $F_2^*(Q^2)$. While the valence quark contributions are obtained by the covariant spectator quark model [23], those of the meson cloud contributions are obtained by the chiral unitary model [25]. Data are from CLAS [51] and MAID [52].

$Q^2 > 1$ GeV^2, since the applicability of the model requires $Q^2 \gg \left(\frac{M_S^2 - M^2}{2M_S}\right)^2 \simeq 0.21$ GeV^2, where M_S corresponds to this case to the $N^*(1535)$ mass [23].

For the $\gamma^* N \to N^*(1535)$ reaction we can observe different roles of the valence quark and meson cloud degrees of freedom. Since in both cases for F_1^* and F_2^* the imaginary part is small, we will focus only on the real part. In Fig. 2 one can notice the dominance of the valence quark effect for the Dirac-type form factor F_1^*, with the prediction very close to the data [51, 52] for $Q^2 > 1$ GeV^2. In this case the meson cloud contributions are about an order of magnitude smaller than those of the valence quarks. As for the Pauli-type form factor F_2^*, one can see, on the other hand, that the meson cloud contributions are sufficient to explain the data for $Q^2 < 1$ GeV^2. Furthermore, the valence and meson cloud contributions have opposite signs with similar magnitude for $Q^2 > 1$ GeV^2. The cancellation between the two contributions may be the main reason of the experimental result, $F_2^* \simeq 0$ for $Q^2 > 1$ GeV^2 (see F_2^* in Fig. 2).

For later convenience, we study also the falloff of the form factors for the valence quark contributions in the large Q^2 region. Apart from logarithm corrections (very smooth variation with Q^2) [23], the falloff behavior of the form factors can be expressed by $F_1^*(Q^2) \approx \left(\frac{\Lambda_1^2}{\Lambda_1^2+Q^2}\right)^2$ and $F_2^*(Q^2) \approx \left(\frac{\Lambda_2^2}{\Lambda_2^2+Q^2}\right)^3$, where $\Lambda_1^2 \simeq 2.6$ GeV^2 and $\Lambda_2^2 \simeq 2.7$ GeV^2 for $Q^2 \simeq 2$ GeV^2. Therefore, the $\gamma^* N \to N^*(1535)$ transition form factors have much slower falloff than that for the nucleon elastic form factors, where the corresponding cutoff is $\Lambda^2 = 0.71$ GeV^2.

We recall that the individual contributions, those from the valence quarks and meson cloud, are based on the different frameworks. The valence quark contributions are estimated by a constituent quark model that takes into account the quark internal electromagnetic structure (including possible quark-antiquark internal excitations), but it does not include the processes where a meson is created by the overall baryon. On the other hand, the meson cloud contributions are estimated in the meson-baryon interactions where both states are considered as structureless particles but modified by monopole meson form factors (see Sec. IV). Due to the differences in the degrees of freedom used in the two approaches described above, we cannot simply combine the individual contributions to get total results for the form factors. However, the opposite signs of the individual contributions for F_2^* are very suggestive, that a strong cancellation between the valence quark and meson cloud effects may take place in a unified approach.

The results shown for the $\gamma^* N \to N(1535)$ reaction suggest that the form factor representation may be very convenient to analyze the transition between the nucleon and the first excited state of the nucleon with a negative parity. Using the form factor representation, it is clear that while F_1^* is dominated by the valence quark contributions, F_2^* may be a result of the competition between the valence quark and meson cloud effects. This simple separation is not obvious in the helicity amplitude representation.

The results obtained for the $\gamma^* N \to N^*(1535)$ reaction, and the simplified interpretation in terms of the individual (valence quarks and meson cloud) contributions, raise a question, namely, whether or not such a trend can be observed for similar reactions. Therefore, we next study the $\gamma^* \Lambda \to \Lambda^*$ $(Y = \Lambda, \Sigma^0)$ reactions with $\Lambda^* = \Lambda(1670)$.

B. $\gamma^* \Lambda \to \Lambda^*$ and $\gamma^* \Sigma^0 \to \Lambda^*$ transition form factors

We now discuss the $\gamma^* Y \to \Lambda^*$ reactions, for $Y = \Lambda$ and Σ^0. As in the previous section we will compare the contributions from the valence quarks and those from the meson cloud dressing for the corresponding form factors. The results of the valence quark contributions derived from the covariant spectator quark model are given in Sec. III [Eqs. (34)-(37)]. The meson cloud contributions

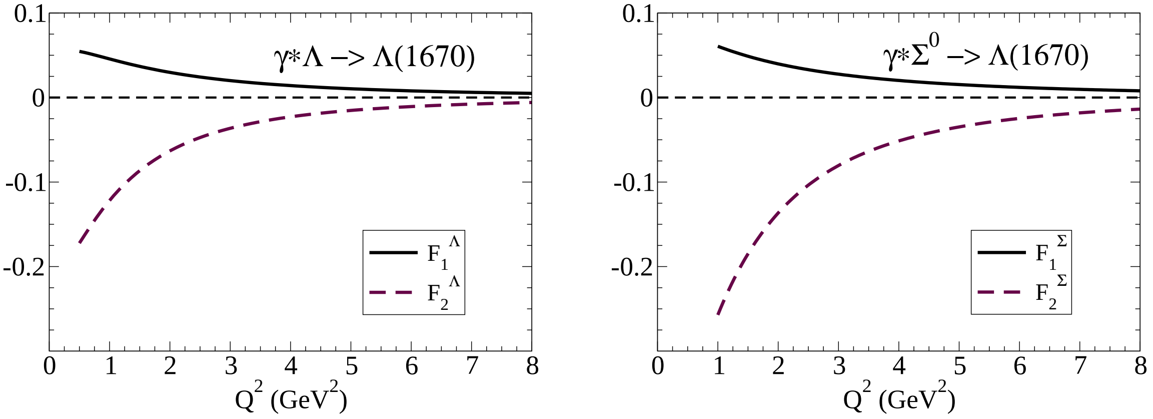

FIG. 3: (Color online) Valence quark contributions for the $\gamma^* Y \to \Lambda(1670)$ form factors, for $Y = \Lambda$ (left panel), and $Y = \Sigma^0$ (right panel).

calculated in Ref. [17] using the chiral unitary model, are reviewed in Sec. IV [Eqs. (51) and (52)].

1. *Results of spectator quark model*

First, we discuss the valence quark contributions, which are presented here for the first time, using the covariant spectator quark model. As mentioned already, the valence quark contributions depend on the two different phases (signs), η_{Λ^*}, the relative sign between the Λ and Λ^* states, and $\eta_{\Lambda\Sigma^0}$ given by the relative sign between the Λ and Σ^0 radial wave function normalization constants. We first consider $\eta_{\Lambda^*} = 1$ case, since it is equivalent to the phase for the $N^*(1535)$-nucleon case as already discussed. The sign was determined by the experimental form factor data[4] [23] (see Fig. 2). As for the reaction involving the Σ^0, we take $\eta_{\Lambda\Sigma^0} = 1$, which is equivalent to state that the Λ and Σ radial wave function normalization constants are both positive.

The results are presented in Fig. 3. The Q^2 region shown is extended up to $Q^2 = 8$ GeV^2, in order to observe better the falloff behavior of the F_1^Y and F_2^Y taking advantage of the covariant nature of the model. We focus on the region $Q^2 > 1$ GeV^2 that satisfies the model applicable condition, $Q^2 \gg 0.2$ GeV^2 for both the reactions, since $|\mathbf{q}|^2_{0Y} \approx 0.2$ GeV^2. We can observe in Fig. 3 the slow falloff for the both form factors in both reactions, particularly for F_1^Y. We will come back later to the falloff of the form factors.

Another interesting point in Fig. 3 is the magnitude of the form factors F_1^Y and F_2^Y which is very similar for the both cases Λ and Σ^0. However, the form factors for the reaction with Σ^0 dominates over the one with Λ in the high Q^2 region. This is particularly noticeable for F_2^Y.

The similarity between the results for $\gamma^*\Lambda \to \Lambda^*$ and $\gamma^*\Sigma^0 \to \Lambda^*$ can be understood by the expressions for the form factors given by Eqs. (34)-(35) and Eqs. (36)-(37). In both cases there is a dependence on the overlap integral $\mathcal{I}_Y$. As the scalar wave functions have the same parametrization for the Λ and Σ^0 the difference in the overlap integrals in their respective rest frames are only due to the masses (M_Λ and M_Σ), leading to almost the same results for both cases. Therefore, the main difference in the form factors comes from the flavor factors that are multiplied by the overlap integrals. Although the flavor factors contain the functions f_{i+}, f_{i-} and f_{i0} ($i = 1, 2$) which are dependent on Q^2, we can make a simple estimate in the exact $SU(3)$ limit taking $f_{i+} = f_{i-} = f_{i0}$ ($i = 1, 2$). In this limit we have $F_i^\Sigma(Q^2) = \sqrt{3} F_i^\Lambda(Q^2)$ ($i = 1, 2$) consistent with the magnitude shown in Fig. 3. We note that our results are different from those in Ref. [53] obtained using a constituent quark model, and also different from those of the chiral unitary model [17] which shows $|F_2^\Sigma| \gg |F_2^\Lambda|$ for $Q^2 \simeq 0$ as seen later. This relation comes from the Λ^* decay widths to $\gamma\,\Lambda$ ($\Gamma_{\gamma\Lambda}$) and $\gamma\,\Sigma^0$ ($\Gamma_{\gamma\Sigma^0}$), which are predicted to be $\Gamma_{\gamma\Sigma^0} \gg \Gamma_{\gamma\Lambda}$ (in general $\Gamma_{\gamma Y} \propto |A^Y_{1/2}(0)|^2 \propto |F_2^Y(0)|^2$). We recall again that the results of the present valence quark model are valid for $Q^2 \gg 0.2$ GeV^2 and the region near $Q^2 = 0$ is excluded, and thus we cannot predict the corresponding decay widths reliably.

We discuss next the rate of the falloff of the form factors, again apart logarithm corrections. We measure the falloff based on $F_1^*(Q^2) \approx \left(\frac{\Lambda_1^2}{\Lambda_1^2 + Q^2}\right)^2$ and $F_2^*(Q^2) \approx \left(\frac{\Lambda_2^2}{\Lambda_2^2 + Q^2}\right)^3$ for $Q^2 \simeq 2$ GeV^2. While for $\gamma^*\Lambda \to \Lambda^*$, we have $\Lambda_1^2 = 3.6$ GeV^2 and $\Lambda_2^2 = 3.6$ GeV^2, for $\gamma^*\Sigma^0 \to \Lambda^*$ we have $\Lambda_1^2 = 3.1$ GeV^2 and $\Lambda_2^2 = 3.2$ GeV^2. In all cases, we have slower falloff than that for the $\gamma^* N \to N^*(1535)$ reaction. Since in the flavor symmetric limit the falloff should be same among the octet baryons, the differences among N and Λ (or Σ^0), and N^* and Λ^*, are a consequence of a special role of the strange quark which breaks flavor symmetry.

---

[4] The sign of the $N^*(1535)$ wave function was adjusted to generate $F_1^*(Q^2) < 0$, in agreement with the data from Refs. [51, 52]. In fact, for F_1^* the valence quark contributions give a very good approximation to describe the data [23, 24].

There are two factors that can cause the slower falloff of the $\gamma^* Y \to \Lambda^*$ transition form factors than the one for the $\gamma^* N \to N^*(1535)$ reaction. The first one is the difference in the quark distributions between the nucleon-$N^*(1535)$ and the $Y - \Lambda^*$ systems. The second one is the difference in the kinematics between the two systems. As for the difference in the quark distributions, Λ and Σ^0 are more compact systems than that of the nucleon, because they have one heavier strange quark in contrast with the nucleon which have only the light quarks. Therefore, the Λ and Σ^0 are characterized by the radial wave functions (18) with a larger extension in the momentum space, and consequently the overlap integral becomes larger than the one for the $\gamma^* N \to N^*(1535)$ reaction. However, this is not the main factor, since the parameters corresponding to the Λ and Σ^0 wave functions are not different significantly from those of the nucleon[5]. The second factor is the difference in the kinematics between the two reactions. For the radial wave functions given by Eq. (18), it is possible to show that the systems with the same parametrization are characterized by the overlap integrals $\mathcal{I}_Y$, which are functions of the ratio $\frac{|\mathbf{q}|_Y}{M_Y}$ (see Appendix B). Therefore, the falloff of $\mathcal{I}_Y$ is determined by the factor $\frac{|\mathbf{q}|_Y}{M_Y}$. The larger the ratio, the falloff is larger. Comparing the values of $\frac{|\mathbf{q}|_\Lambda}{M_\Lambda}$ with the corresponding ratio $\frac{|\mathbf{q}|}{M}$ for the $\gamma^* N \to N^*(1535)$ reaction, the latter has the larger ratio for $Q^2 = 0$ ($\frac{|\mathbf{q}|}{M} = 0.48$ compared with $\frac{|\mathbf{q}|_\Lambda}{M_\Lambda} = 0.41$) and this is true for also for larger values of Q^2. This means the overlap integral has stronger falloff for the $\gamma^* N \to N^*(1535)$, and it is reflected on the faster falloff of the form factors.

To compare the falloff for the reactions $\gamma^* \Lambda \to \Lambda^*$ and $\gamma^* \Sigma^0 \to \Lambda^*$, we need to analyze more in detail to explain the difference in the observed behavior, namely, the falloff for the reaction involving Σ^0 is faster (smaller cutoffs) than that for the reaction involving Λ. In this case the ratios $\frac{|\mathbf{q}|_Y}{M_Y}$ are close, $\frac{|\mathbf{q}|_\Lambda}{M_\Lambda} = 0.41$ and $\frac{|\mathbf{q}|_\Sigma}{M_\Sigma} = 0.36$, for $Q^2 = 0$. The important effect now is the contribution from the flavor factors in the form factors, given by Eqs. (34)-(35) and (36)-(37). The form factors for the reaction involving the Λ have dependence on the strange quark form factors f_{10} and f_{20}, and that these functions have slower falloff with Q^2 than those with the reaction involving the Σ^0, which depend only on the light quark form factors. Then, the corresponding transition form factors for the reaction with Λ also have slower falloff than that for the reaction with Σ^0.

2. *Results of chiral unitary model*

Next we show the result of the transition form factors calculated in the chiral unitary model. In Figs. 4 and 5, we show the results of the Dirac- and Pauli-type form factors, $F_1^Y(Q^2)$ and $F_2^Y(Q^2)$, for the $\gamma^* Y \to \Lambda^*$ transition, respectively. As seen in the figures, in the meson cloud model the F_2^Y form factors for both cases are one order of magnitude larger than the F_1^Y form factors. This is very similar tendency as that for the $N(1535)$ case.

In Figs. 4 and 5 we also show the contribution coming from each meson separately. For the Λ transition form factors the pion contribution is very small. This is because only the isoscalar component of the photon current can contribute the $\gamma^* \Lambda \to \Lambda^*$ transition in the isospin symmetric limit, while the pion with isospin 1 can couple only to the isovector part of the photon current. Thus, with very small isospin breaking effect there is little pion cloud contribution in the $\gamma^* \Lambda \to \Lambda^*$ transition. It is also interesting to mention that for the $\gamma^* \Lambda \to \Lambda^*$ transition there is cancellation between K^- and K^+ contributions, while the $\gamma^* \Sigma^0 \to \Lambda^*$ transition is dominated by the K^+ cloud component. In this way, for the both form factors F_1^Y and F_2^Y, the transition from Σ^0 is larger than that from Λ. Especially for the Pauli-type form factor, F_2^Σ is almost seven times larger than F_2^Λ. This cancellation is also found for the helicity amplitudes (see Ref. [17] for the details).

3. *Comparison of two models*

Finally, we compare the valence quark contributions with those from the meson cloud for the reactions involving the Λ and Σ^0. The comparison is shown in Fig. 6, for the reactions involving the Λ (left panel) and the Σ^0 (right panel). Note that the chiral unitary model results have both the real and imaginary parts and the absolute phases are fixed at $Q^2 = 0$ to give a real and positive value of $A_{1/2}^Y(0)$, or equivalently real and negative $F_2^Y(0)$, as mentioned before.

One can see in Fig. 6 that the imaginary part is small in general. Therefore, we will focus only on the real part hereafter. Another interesting point is that, while the both form factors for the reaction involving the Λ are dominated by the valence quark contributions, this is not the case for the reaction involving the Σ^0. For the latter case one can see that the valence quark contributions for F_1^Σ are larger than those from the meson cloud (about 2.5 times near $Q^2 = 2.5$ GeV^2), although the magnitude is similar for F_2^Σ.

A point of particular importance about F_2^Σ is the relative sign between the valence and meson cloud contributions. Since, as mentioned before, the factor $\eta_{\Lambda\Sigma^0}$ is

---

[5] While the Λ and Σ^0 radial wave functions are characterized by the parameter $\beta_3 \simeq 0.76$ [28], that of the nucleon system is parameterized by $\beta_2 \simeq 0.72$ [27] (smaller momentum scale). In both cases the additional range parameter is $\beta_1 \approx 0.05$ [27, 28].

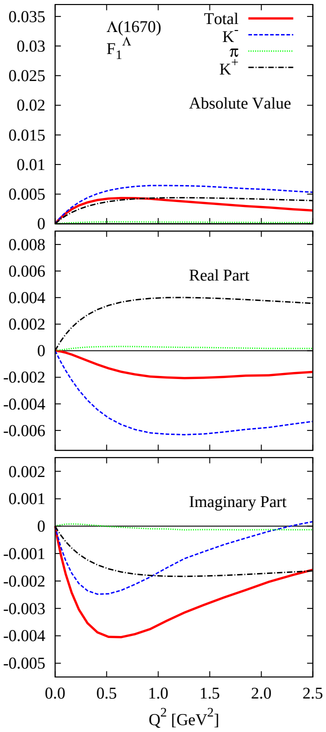

FIG. 4: (Color online) Meson cloud contributions for the Dirac-type form factor $F_1^Y(Q^2)$ of the $\gamma^* Y \to \Lambda^*$ transition for $Y = \Lambda$ (left panels) and $Y = \Sigma^0$ (right panels). The solid line shows the total contribution coming from diagram (a), while the dashed, dotted and dot-dashed lines denote the K^-, π and K^+ contributions, respectively.

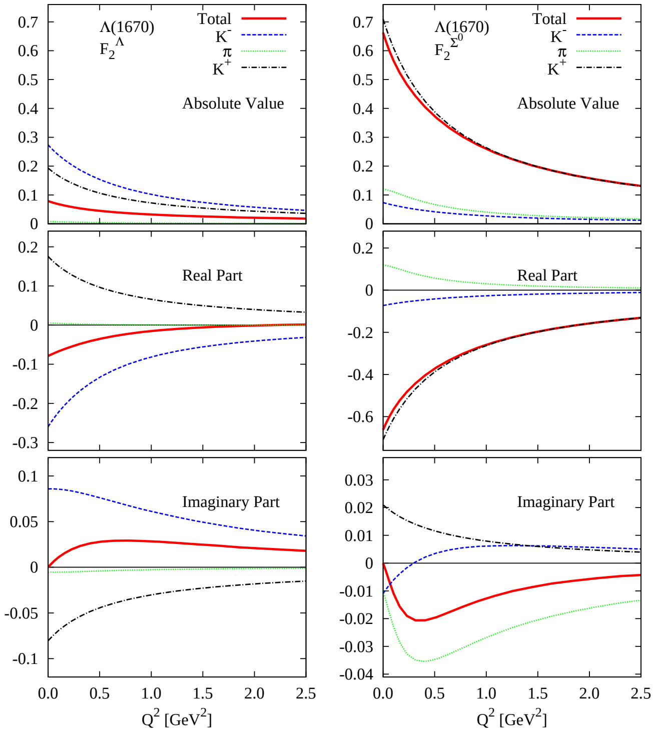

FIG. 5: (Color online) Meson cloud contributions for the Pauli-type form factor $F_2^Y(Q^2)$ of the $\gamma^* Y \to \Lambda^*$ transition for $Y = \Lambda$ (left panels) and $Y = \Sigma^0$ (right panels). The solid line shows the total contribution coming from diagram (a), while the dashed, dotted and dot-dashed lines denote the K^-, π and K^+ contributions, respectively.

unknown at present, we cannot decide if there is a positive or negative interference between the contributions. The results for the form factors involving the Σ^0 are determined using $\eta_{\Lambda^*}\eta_{\Lambda\Sigma^0} = 1$. If this is the case, there is a combination of the signs to enhance the total magnitude of F_2^Σ. On the other hand, if the sign is opposite, $\eta_{\Lambda^*}\eta_{\Lambda\Sigma^0} = -1$, one can expect a cancellation between the valence quark and meson cloud effects, leading to a result $F_2^\Sigma \approx 0$, or to a magnitude similar to F_1^Σ. An example of a quark model with $F_2^\Sigma > 0$ can be found in Refs. [53, 54]. Note that in case $\eta_{\Lambda^*}\eta_{\Lambda\Sigma^0} = -1$, the reaction $\gamma^*\Sigma^0 \to \Lambda^*$ has similar properties with the reaction $\gamma^* N \to N^*(1535)$, discussed previously. This result suggests that the experimental determination of the sign for F_2^Σ is very important to pin down the relative phase between the Λ and Σ^0 wave functions in the present model as we explain next.

From the discussions above, we conclude that, if $\eta_{\Lambda^*}\eta_{\Lambda\Sigma^0} = +1$, it is expected that F_2^Σ becomes larger in magnitude. In the alternative case, $\eta_{\Lambda^*}\eta_{\Lambda\Sigma^0} = -1$, F_2^Σ should be smaller in magnitude, and comparable with F_1^Σ. Therefore, once the sign η_{Λ^*} is known, $\eta_{\Lambda\Sigma^0}$ can be inferred from the result for F_2^Σ. Note also that in our model η_{Λ^*} can be fixed by the results for the reaction $\gamma^*\Lambda \to \Lambda^*$, since valence quark effect dominates that transition ($F_1^\Sigma \propto \eta_{\Lambda^*}$). Then $\gamma^*\Lambda \to \Lambda^*$ can be used to determine $\eta_{\Lambda\Sigma^0}$, which fixes also the sign of $\mu_{\Lambda\Sigma^0}$.

The covariant spectator quark model can also be used to calculate the valence quark contributions for the $\gamma^*\Lambda \to \Sigma^0$ form factors in general and the transition magnetic moment $\mu_{\Lambda\Sigma^0}$ in particular. Assuming that the valence quark effect is the leading contribution as demonstrated reasonable for the octet baryon system [28], one can conclude that $\mu_{\Lambda\Sigma^0} \propto -\eta_{\Lambda\Sigma^0}$ [48], namely, the sign of $\mu_{\Lambda\Sigma^0}$ is the opposite to that of $\eta_{\Lambda\Sigma^0}$. Thus, once determined the sign of $\eta_{\Lambda\Sigma^0}$ corresponding to the reaction $\gamma^*\Sigma^0 \to \Lambda^*$, we can determine the sign of $\mu_{\Lambda\Sigma^0}$.

For completeness, we also present in Fig. 7 the results for the helicity amplitudes $A_{1/2}^Y$ and $S_{1/2}^Y$ converted from F_1^Y and F_2^Y by Eqs. (6) and (7), assuming the same phases as the form factors[6]. For the $\gamma^*\Lambda \to \Lambda^*$ reaction we can also observe the dominance of the valence quark contributions over the meson cloud contributions. As for the $\gamma^*\Sigma^0 \to \Lambda^*$ reaction, the more interesting point is the closeness of the valence and meson cloud contributions for the $S_{1/2}^\Sigma$ amplitude. Also in this case we can conclude that if $\eta_{\Lambda^*}\eta_{\Lambda\Sigma^0} = +1$, $S_{1/2}^\Sigma$ is enhanced, while

---

[6] The $A_{1/2}^Y$ helicity amplitude shown in Ref. [17] has a different absolute phase from the present work.

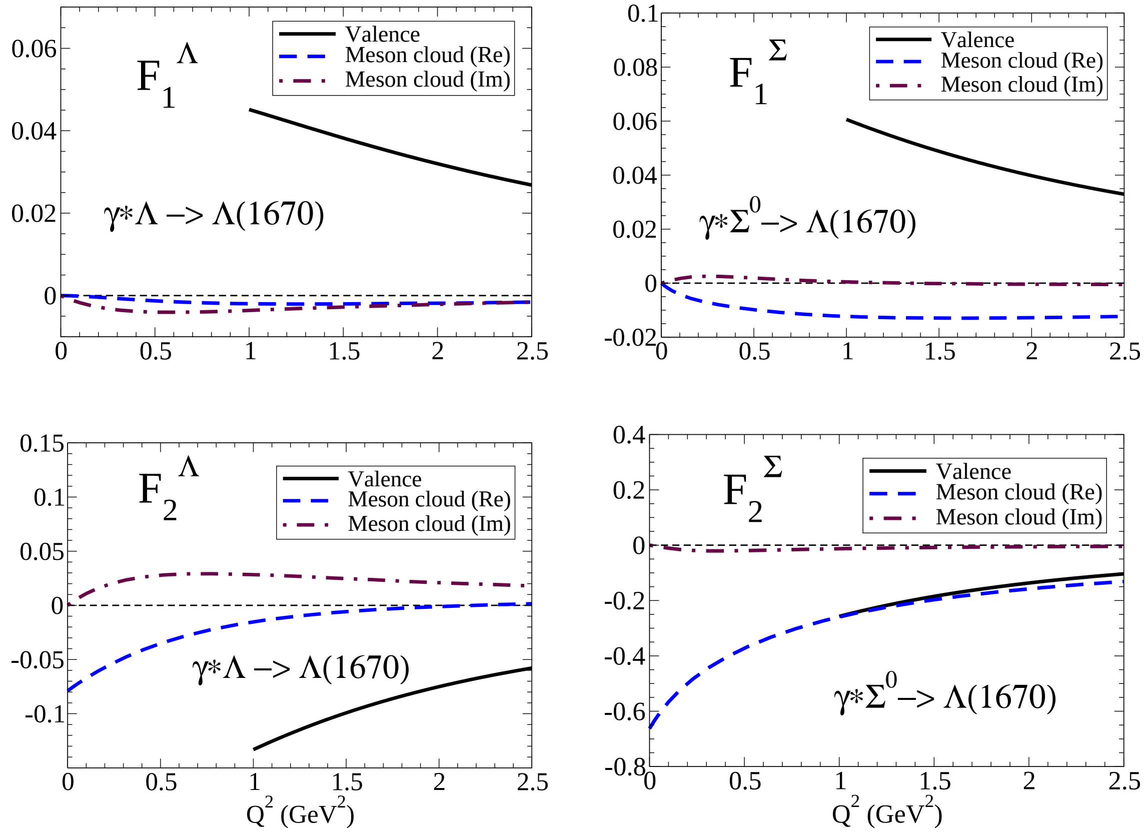

FIG. 6: (Color online) Valence quark and meson cloud contributions for the $\gamma^* Y \to \Lambda^*$ transition form factors for $Y = \Lambda$ (left panel), and $Y = \Sigma^0$ (right panel).

the alternative case, $\eta_{\Lambda^*}\eta_{\Lambda\Sigma^0} = -1$, we expect a substantial reduction of the $S_{1/2}^{\Sigma}$ amplitude. The similarity in the behavior for $S_{1/2}^{\Sigma}$ and F_2^{Σ}, as discussed before, is a consequence of the partial suppression of the F_1^* contribution for the $S_{1/2}^{\Sigma}$ amplitude, due to the factor $\frac{M_{\Lambda^*}-M_Y}{M_{\Lambda^*}+M_Y}$. Another interesting point in Fig. 7 is the flatness of the valence quark model result for $A_{1/2}^{Y}$ as a function of Q^2 around the region $Q^2 = 2$ GeV^2. This is because the region $Q^2 = 2$ GeV^2 is the turning point of changing the Q^2 dependence in the amplitude. For the larger Q^2 region however, the expected falloff with the Q^2 can be observed.

VI. CONCLUSIONS

In this study we have analyzed the contributions from the valence quark and meson cloud effects for the $\gamma^* B \to B^*$ reactions with $B = N, \Lambda, \Sigma^0$ and $B^* = N(1535), \Lambda(1670)$. While the valence quark contributions are estimated using a constituent quark model [23, 27, 28], those of the meson cloud are estimated using the chiral unitary model [17, 25]. In the chiral unitary model, the $N(1535)$ has some components other than meson-baryon dynamics as discussed in Ref. [13], but for the calculation of the transition form factors we take only coupling of the photon current to the meson component and do not take into account of photon couplings to genuine quark components. In this approach the $\Lambda(1670)$ is almost composed of meson-baryon components [17]. Since the valence and meson cloud effects are calculated by the different formalisms we cannot simply combine the both contributions to obtain the final, total results for the transition form factors. Nevertheless, the magnitude and signs of the individual contributions presented here are sufficient to conclude that it is possible to have a cancellation from the two effects, the valence quark and meson cloud effects, in a consistent, unified approach including the both effects.

For the $\gamma^* N \to N^*(1535)$ reaction, we have found difference in signs for the two contributions for the Pauli-type form factor F_2^*, which can be the main reason for the experimental observation, $F_2^* \simeq 0$ for $Q^2 > 2$ GeV^2.

As for the reactions $\gamma^* Y \to \Lambda(1670)$ $(Y = \Lambda, \Sigma^0)$, we conclude that generally the valence quark contributions dominate for the $Y = \Lambda$ case, but the two contributions are similar for the reaction with $Y = \Sigma^0$. A particularly interesting case is the form factor F_2^{Σ}. Namely, if we assume the same sign for the Λ and Σ radial wave function normalization constants ($\eta_{\Lambda\Sigma^0} = 1$) and $\eta_{\Lambda^*} = 1$,

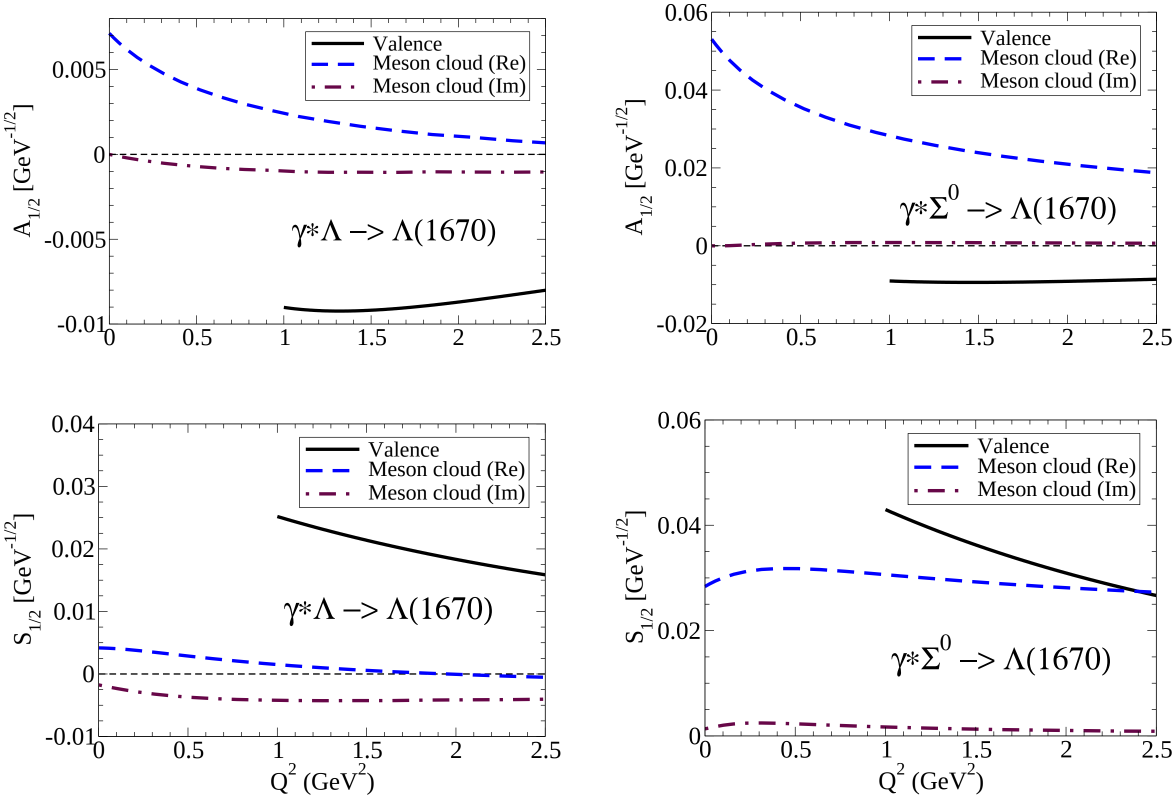

FIG. 7: (Color online) Valence quark and meson cloud contributions for the $\gamma^* Y \to \Lambda^*$ helicity amplitudes for $Y = \Lambda$ (left panel) and $Y = \Sigma^0$ (right panel).

we have an enhancement for F_2^Σ. Instead, if we assume $\eta_{\Lambda^*}\eta_{\Lambda\Sigma^0} = -1$, we have a substantial cancellation between the two effects. Then, the F_2^Σ contribution for the reaction cross section would be very small.

A consequence of the observation made above is that the $\gamma^*\Sigma^0 \to \Lambda^*$ reaction can provide an indirect method to determine $\eta_{\Lambda\Sigma^0}$, which can be used to pin down the sign of $\mu_{\Lambda\Sigma^0}$ consistently within the present approach. This can be of fundamental importance, because the sign of the $\gamma^*\Lambda \to \Sigma^0$ transition form factors, and in particular the sign of the transition magnetic moment, $\mu_{\Lambda\Sigma^0}$, is not determined experimentally. Also this sign has not been related consistently with the other reactions so far. Although the sign is predicted to be negative within the unitary symmetry approach [55] (the same sign with the neutron magnetic moment), the consistency with other reaction was not studied within the approach.

From the discussion made above we conclude that the theoretical and experimental studies of the reactions $\gamma^* N \to N^*(1535)$ and $\gamma^* Y \to \Lambda^*$, with $Y = \Lambda, \Sigma^0$, as well as the correlations between them, are very interesting topics of investigation. The results from these transition form factors can be used to estimate the light and strange quark distributions in the baryons, as well as to predict other reactions.

Acknowledgments

G. R. acknowledges CSSM, the University of Adelaide for making him possible to visit and stay, and thank A. W. Thomas and H. Kamano for helpful discussions. D. J. would like to thank M. Doring and E. Oset for the collaboration on the helicity amplitudes in the chiral unitary model. This work was partially financed by the European Union (HadronPhysics2 project "Study of strongly interacting matter") and by the Fundação para a Ciência e a Tecnologia, under Grant No. PTDC/FIS/113940/2009, "Hadron structure with relativistic models", and partially supported by the Grants-in-Aid for Scientific Research (No. 22740161 and No. 22105507), and carried out in part under the Yukawa International Program for Quark- hadron Sciences (YIPQS). This work was also supported by the University of Adelaide and the Australian Research Council through grant No. FL0992247 (AWT). G. R. was supported by the Fundação para a Ciência e a Tecnologia under the Grant No. SFRH/BPD/26886/2006.

Appendix A: Current matrix elements in the covariant spectator quark model

The calculation of the matrix elements for a transition between a $J^P = \frac{1}{2}^+$ initial state and a $J^P = \frac{1}{2}^-$ final state follows the same steps as that of Appendix B in Ref. [23] for the $\gamma^* N \to N(1535)$ reaction. Here it is sufficient to note that in the transition current involving the Ψ_{Λ^*} the terms in $(\varepsilon_\pm \cdot \tilde{k})$ vanish in the k integral. Therefore, only the terms proportional to the integral

$$\mathcal{I}_Y = -\eta_{\Lambda^*} \int_k N(\varepsilon_0 \cdot \tilde{k}) \psi_{\Lambda^*} \psi_Y, \tag{A1}$$

survive in the current. The minus sign is introduced for convenience.

With this simplification we can derive the following results,

$$\int_k \left[\overline{\Phi}_\rho \hat{\gamma}^\mu \phi_S^0\right] \psi_{\Lambda^*}\psi_Y = -\mathcal{I}_Y \left\{\bar{u}_{\Lambda^*} \hat{\gamma}^\mu \gamma_5 u_Y\right\}, \tag{A2}$$

$$\int_k \left[\overline{\Phi}_\rho \frac{i\sigma^{\mu\nu} q_\nu}{2M} \phi_S^0\right] \psi_{\Lambda^*}\psi_Y = \mathcal{I}_Y \left\{\bar{u}_{\Lambda^*} \frac{i\sigma^{\mu\nu} q_\nu}{2M} \gamma_5 u_Y\right\}, \tag{A3}$$

$$\int_k \left[\overline{\Phi}_\lambda \hat{\gamma}^\mu \phi_S^1\right] \psi_{\Lambda^*}\psi_Y = \frac{1}{3}\mathcal{I}_Y \left\{\bar{u}_{\Lambda^*} \hat{\gamma}^\mu \gamma_5 u_Y\right\}, \tag{A4}$$

$$\int_k \left[\overline{\Phi}_\lambda \frac{i\sigma^{\mu\nu} q_\nu}{2M} \phi_S^1\right] \psi_{\Lambda^*}\psi_Y = -\frac{1}{3}\mathcal{I}_Y \left\{\bar{u}_{\Lambda^*} \frac{i\sigma^{\mu\nu} q_\nu}{2M} \gamma_5 u_Y\right\} \tag{A5}$$

Inserting these results into the expression of the current, we obtain

$$\begin{aligned} J_Y^\mu &= +e\,\frac{1}{2}(3 j_1^A + j_1^S) \mathcal{I}_Y \; \hat{\gamma}^\mu \gamma_5 \\ &\quad -e\,\frac{1}{2}(3 j_2^A - j_2^S) \mathcal{I}_Y \; \frac{i\sigma^{\mu\nu} q_\nu}{2M} \gamma_5. \end{aligned} \tag{A6}$$

Appendix B: Overlap integral

Consider the overlap integral in the final state (Λ^*) rest frame, given by Eq. (38), with the radial wave functions of Eq. (18),

$$\begin{aligned} \mathcal{I}_Y(Q^2) &= \eta_{\Lambda^*} \frac{\mathcal{N}_\Lambda \mathcal{N}_Y}{m_D^2} \int_k \frac{k_z}{|\mathbf{k}|} \left\{ \frac{1}{(\beta_1 + \chi_{\Lambda^*})(\beta_3 + \chi_{\Lambda^*})} \right. \\ &\quad \left. \times \frac{1}{(\beta_1 + \chi_Y)(\beta_3 + \chi_Y)} \right\}. \end{aligned} \tag{B1}$$

In the above equation χ_B is determined by Eq. (17) for the momenta defined by Eq. (39). Therefore,

$$\chi_{\Lambda^*} = 2\left(\frac{E_D}{m_D} - 1\right), \tag{B2}$$

and

$$\chi_Y = 2\left(\frac{E_Y}{M_Y}\frac{E_D}{m_D} + \frac{|\mathbf{q}|_Y}{M_Y} k_z - 1\right), \tag{B3}$$

where

$$\frac{E_Y}{M_Y} = \sqrt{1 + \frac{|\mathbf{q}_Y|^2}{M_Y^2}}. \tag{B4}$$

From Eq. (B2) we can see that χ_{Λ^*} has no dependence on Q^2 (or $|\mathbf{q}|_Y$), and that from Eq. (B3) χ_Y is a function of the ratio $\frac{|\mathbf{q}|_Y}{M_Y}$. Therefore, we can write

$$\mathcal{I}_Y(Q^2) = \mathcal{I}_Y\left(\frac{|\mathbf{q}|_Y}{M_Y}\right). \tag{B5}$$

Furthermore, since χ_Y increases when $\frac{|\mathbf{q}|_Y}{M_Y}$ increases, we can conclude that the absolute value of the integrand function in Eq. (B1) decreases with $\frac{|\mathbf{q}|_Y}{M_Y}$ for a given $\mathbf{k}$, and therefore $|\mathcal{I}_Y|$ decreases when the ratio $\frac{|\mathbf{q}|_Y}{M_Y}$ increases. These results show that, when we have two reactions described by the same radial wave function (the same values for the parameters β_1 and β_3), the reaction with larger ratio $\frac{|\mathbf{q}|_Y}{M_Y}$ for a given Q^2, gets the smaller value for $|\mathcal{I}_Y|$.

A simple consequence of the above result applies for the nucleon-$N^*(1535)$ and $\Lambda - \Lambda^*$ transition form factors, when the wave functions are parameterized exactly the same, $\frac{|\mathbf{q}|}{M}$ for the nucleon case is larger than $\frac{|\mathbf{q}|_\Lambda}{M_\Lambda}$ for the Λ case, and we have,

$$|\mathcal{I}_\Lambda(Q^2)| > |\mathcal{I}_N(Q^2)|. \tag{B6}$$

This relation also explains the faster falloff of the $\gamma^* N \to N^*(1535)$ transition form factors than that of the $\gamma^* \Lambda \to \Lambda^*$ transition form factors.

---

[1] K. Nakamura *et al.* [Particle Data Group], J. Phys. G **37**, 075021 (2010).

[2] R. H. Dalitz, S. F. Tuan, Annals Phys. **10**, 307-351 (1960).

[3] R. H. Dalitz, T. C. Wong, G. Rajasekaran, Phys. Rev. **153**, 1617-1623 (1967).

[4] H. W. Wyld, Phys. Rev. **155**, 1649-1662 (1967).

[5] N. Kaiser, P. B. Siegel and W. Weise, Nucl. Phys. A **594**, 325 (1995) [arXiv:nucl-th/9505043].

[6] N. Isgur, G. Karl, Phys. Rev. **D18**, 4187 (1978).

[7] J. W. Darewych, M. Horbatsch and R. Koniuk, Phys. Rev. D **28**, 1125 (1983).

[8] S. Capstick and W. Roberts, Prog. Part. Nucl. Phys. **45**, S241 (2000) [arXiv:nucl-th/0008028].

[9] E. A. Veit, B. K. Jennings, A. W. Thomas and R. C. Barrett, Phys. Rev. D **31**, 1033 (1985).

[10] E. Oset and A. Ramos, Nucl. Phys. **A635**, 99 (1998).

[11] D. Jido, J. A. Oller, E. Oset, A. Ramos and U. G. Meissner, Nucl. Phys. A **725**, 181 (2003) [arXiv:nucl-th/0303062].

[12] T. Hyodo and W. Weise, Phys. Rev. **C77**, 035204 (2008).

[13] T. Hyodo, D. Jido, and A. Hosaka, Phys. Rev. **C78**, 025203 (2008).

[14] T. Hyodo and D. Jido, Prog. Part. Nucl. Phys. **67**, 55 (2012) [arXiv:1104.4474 [nucl-th]].

[15] M. Doring, J. Haidenbauer, U. G. Meissner and A. Rusetsky, arXiv:1108.0676 [hep-lat].

[16] Y. Ikeda, T. Hyodo, D. Jido, H. Kamano, T. Sato and K. Yazaki, Prog. Theor. Phys. **125**, 1205 (2011) [arXiv:1101.5190 [nucl-th]].

[17] M. Doring, D. Jido and E. Oset, Eur. Phys. J. A **45**, 319 (2010) [arXiv:1002.3688 [nucl-th]].

[18] E. Oset, A. Ramos, and C. Bennhold, Phys. Lett. **B527**, 99 (2002).

[19] J. A. Oller and Ulf G. Meissner, Phys. Lett. **B500**, 263 (2001).

[20] D. B. Leinweber, Annals Phys. **198**, 203 (1990).

[21] C. S. An, B. Saghai, S. G. Yuan and J. He, Phys. Rev. C **81**, 045203 (2010) [arXiv:1002.4085 [nucl-th]].

[22] B. J. Menadue, W. Kamleh, D. B. Leinweber and M. S. Mahbub, arXiv:1109.6716 [hep-lat].

[23] G. Ramalho and M. T. Peña, Phys. Rev. D **84**, 033007 (2011) [arXiv:1105.2223 [hep-ph]].

[24] G. Ramalho and K. Tsushima, Phys. Rev. D **84**, 051301 (2011) [arXiv:1105.2484 [hep-ph]].

[25] D. Jido, M. Döring and E. Oset, Phys. Rev. C **77**, 065207 (2008).

[26] I. G. Aznauryan and V. D. Burkert, Prog. Part. Nucl. Phys. **67**, 1 (2012) [arXiv:1109.1720 [hep-ph]].

[27] F. Gross, G. Ramalho and M. T. Peña, Phys. Rev. C **77**, 015202 (2008) [arXiv:nucl-th/0606029].

[28] G. Ramalho and K. Tsushima, Phys. Rev. D **84**, 054014 (2011) [arXiv:1107.1791 [hep-ph]].

[29] G. Ramalho, F. Gross, M. T. Peña and K. Tsushima, in *Proceedings of the 4th Workshop on Exclusive Reactions at High Momentum Transfer, 2011*, edited by Anatoly Radyushkin (World Scientific, Singapore, 2011), p. 287 [arXiv:1008.0371 [hep-ph]].

[30] F. Gross, Phys. Rev. **186**, 1448 (1969); F. Gross, J. W. Van Orden and K. Holinde, Phys. Rev. C **45**, 2094 (1992).

[31] A. Stadler, F. Gross and M. Frank, Phys. Rev. C **56**, 2396 (1997) [arXiv:nucl-th/9703043].

[32] F. Gross, G. Ramalho and M. T. Peña, arXiv:1201.6337 [hep-ph].

[33] G. Ramalho, K. Tsushima and F. Gross, Phys. Rev. D **80**, 033004 (2009) [arXiv:0907.1060 [hep-ph]].

[34] F. Gross, G. Ramalho and M. T. Peña, arXiv:1201.6336 [hep-ph].

[35] G. Ramalho and M. T. Peña, J. Phys. G **36**, 115011 (2009) [arXiv:0812.0187 [hep-ph]].

[36] G. Ramalho and M. T. Peña, Phys. Rev. D **80**, 013008 (2009) [arXiv:0901.4310 [hep-ph]].

[37] G. Ramalho, M. T. Peña and F. Gross, Phys. Rev. D **78**, 114017 (2008) [arXiv:0810.4126 [hep-ph]].

[38] G. Ramalho, M. T. Peña and F. Gross, Phys. Lett. B **678**, 355 (2009) [arXiv:0902.4212 [hep-ph]].

[39] G. Ramalho, M. T. Peña and F. Gross, Phys. Rev. D **81**, 113011 (2010) [arXiv:1002.4170 [hep-ph]].

[40] G. Ramalho, M. T. Peña and F. Gross, Eur. Phys. J. A **36**, 329 (2008) [arXiv:0803.3034 [hep-ph]].

[41] F. Gross, G. Ramalho and K. Tsushima, Phys. Lett. B **690**, 183 (2010) [arXiv:0910.2171 [hep-ph]].

[42] G. Ramalho and M. T. Peña, Phys. Rev. D **83**, 054011 (2011).

[43] G. Ramalho and K. Tsushima, Phys. Rev. D **81**, 074020 (2010) [arXiv:1002.3386 [hep-ph]].

[44] G. Ramalho and K. Tsushima, Phys. Rev. D **82**, 073007 (2010) [arXiv:1008.3822 [hep-ph]].

[45] F. Gross, G. Ramalho and M. T. Peña, Phys. Rev. C **77**, 035203 (2008).

[46] J. J. Kelly, Phys. Rev. C **56**, 2672 (1997).

[47] Z. Batiz and F. Gross, Phys. Rev. C **58**, 2963 (1998) [arXiv:nucl-th/9803053].

[48] G. Ramalho and K. Tsushima, in preparation.

[49] D. N. Tovee *et al,*, Nucl. Phys. **B33**, 493 (1971).

[50] R. J. Nowak *et al.*, Nucl. Phys. **B139**, 61 (1978).

[51] I. G. Aznauryan *et al.* [CLAS Collaboration], Phys. Rev. C **80**, 055203 (2009) [arXiv:0909.2349 [nucl-ex]].

[52] D. Drechsel, S. S. Kamalov and L. Tiator, Eur. Phys. J. A **34**, 69 (2007) [arXiv:0710.0306 [nucl-th]].

[53] T. Van Cauteren, J. Ryckebusch, B. Metsch and H. R. Petry, Eur. Phys. J. A **26**, 339 (2005) [arXiv:nucl-th/0509047].

[54] T. Van Cauteren, D. Merten, T. Corthals, S. Janssen, B. Metsch, H. R. Petry and J. Ryckebusch, Eur. Phys. J. A **20**, 283 (2004) [arXiv:nucl-th/0310058].

[55] S. R. Coleman and S. L. Glashow, Phys. Rev. Lett. **6**, 423 (1961).